JBC RESEARCH ARTICLE

Disrupting the plastidic iron-sulfur cluster biogenesis pathway in *Toxoplasma gondii* has pleiotropic effects irreversibly impacting parasite viability

Received for publication, April 13, 2022, and in revised form, June 29, 2022 Published, Papers in Press, July 8, 2022,
https://doi.org/10.1016/j.jbc.2022.102243

Eléa A. Renaud[1,‡], Sarah Pamukcu[1,‡], Aude Cerutti[1], Laurence Berry[1], Catherine Lemaire-Vieille[2], Yoshiki Yamaryo-Botté[2], Cyrille Y. Botté[2], and Sébastien Besteiro[1,*]

From the [1]LPHI, University of Montpellier, CNRS, UMR5235, Montpellier, France; [2]ApicoLipid Team, Centre National de la Recherche Scientifique, Institute for Advanced Biosciences, Institut National de la Santé et de la Recherche Médicale, UMR5309, U1209, Université Grenoble Alpes, Grenoble, France

Edited by Ronald Wek

Like many other apicomplexan parasites, *Toxoplasma gondii* contains a plastid harboring key metabolic pathways, including the sulfur utilization factor (SUF) pathway that is involved in the biosynthesis of iron-sulfur clusters. These cofactors are crucial for a variety of proteins involved in important metabolic reactions, potentially including plastidic pathways for the synthesis of isoprenoid and fatty acids. It was shown previously that impairing the NFS2 cysteine desulfurase, involved in the first step of the SUF pathway, leads to an irreversible killing of intracellular parasites. However, the metabolic impact of disrupting the pathway remained unexplored. Here, we generated another mutant of this pathway, deficient in the SUFC ATPase, and investigated in details the phenotypic consequences of TgNFS2 and TgSUFC depletion on the parasites. Our analysis confirms that *Toxoplasma* SUF mutants are severely and irreversibly impacted in division and membrane homeostasis, and suggests a defect in apicoplast-generated fatty acids. However, we show that increased scavenging from the host or supplementation with exogenous fatty acids do not fully restore parasite growth, suggesting that this is not the primary cause for the demise of the parasites and that other important cellular functions were affected. For instance, we also show that the SUF pathway is key for generating the isoprenoid-derived precursors necessary for the proper targeting of GPI-anchored proteins and for parasite motility. Thus, we conclude plastid-generated iron-sulfur clusters support the functions of proteins involved in several vital downstream cellular pathways, which implies the SUF machinery may be explored for new potential anti-*Toxoplasma* targets.

Apicomplexan parasites are some of the most prevalent and morbidity-causing pathogens worldwide. Noticeably, they comprise *Plasmodium* species that can naturally infect humans and cause the deadly malaria in tropical and subtropical areas of the world (1). Although less lethal, another apicomplexan parasite called *Toxoplasma gondii* can cause serious illness in animals, including humans, and has a widespread host range and geographical distribution (2). These protists are obligate intracellular parasites that rely to a large extent on their host cells for nutrient acquisition and for protection from the immune system. Through their evolutionary history, *Plasmodium* and *Toxoplasma* have inherited a plastid from a secondary endosymbiosis event involving the engulfment of a red alga whose photosynthetic capability previously originated from the acquisition of a cyanobacterium (3). Although the ability to perform photosynthesis has been lost during evolution when the ancestors of Apicomplexa became parasitic (4), the plastid has retained critical metabolic functions. For instance, it hosts pathways for the synthesis of heme (together with the mitochondrion), fatty acids (FAs, *via* a prokaryotic FASII (type II fatty acid synthase) pathway), isoprenoid precursors (through the so-called non-mevalonate or 1-deoxy-D-xylulose 5-phosphate pathway), and iron-sulfur (Fe-S) clusters (5, 6). Because of its origin and its metabolic importance, the apicoplast is particularly attractive to look for potential drug targets (7). For example, drugs inhibiting translation in prokaryotic-like systems like clindamycin or doxycycline, which are used for prophylaxis or treatment of Apicomplexa-caused diseases, primarily target the apicoplast (8, 9).

As some of the earliest catalytic cofactors on earth (10), Fe-S clusters are found in all kingdoms of life, associated with proteins involved in a number of key cellular functions like the synthesis of metabolites, the replication and repair of DNA, the biogenesis of ribosomes, and the modification of tRNAs (11). The biosynthesis of Fe-S clusters necessitates a complex machinery for assembling ferrous (Fe^{2+}) or ferric (Fe^{3+}) iron and sulfide (S^{2-}) ions, and delivering the resulting Fe-S cluster to target client proteins (12). In eukaryotes, Fe-S proteins are present in various subcellular compartments like the cytosol and the nucleus, but also in organelles of endosymbiotic origin like mitochondria or plastids, and thus require compartment-specific biogenesis systems. The three main eukaryotic Fe-S synthesis pathways comprise the iron-sulfur cluster (ISC) machinery, hosted by the mitochondrion, the cytosolic iron-sulfur cluster assembly

‡ These authors contributed equally to this work; author order was determined randomly.
* For correspondence: Sébastien Besteiro, sebastien.besteiro@inserm.fr.

machinery, important not only for the generation of cytosolic but also of nuclear Fe-S proteins, and the SUF (sulfur utilization factor) pathway that is found in plastids (11).

Like in plants and algae, apicoplast-containing apicomplexan parasites seem to express the machinery corresponding to the three eukaryotic pathways. For instance, recent investigations in *T. gondii* have shown that the cytosolic iron-sulfur cluster assembly, ISC, and SUF pathways are all essential for parasite fitness (13, 14). From a biochemical point of view, mitochondrial and plastidic Fe-S cluster biosynthesis pathways follow a similar general pattern: cysteine desulfurases produce sulfur from L-cysteine, then scaffold proteins provide a molecular platform allowing assembly of iron and sulfur into a cluster, and finally carrier proteins deliver the cluster to target apoproteins. Importantly, targeting the *T. gondii* mitochondrial ISC pathway through disruption of scaffold protein ISU1 was shown to lead to a reversible growth arrest and to trigger differentiation into a stress-resistant form; while on the other hand, targeting the plastidic SUF pathway by inactivating NFS2 function led to an irreversible lethal phenotype (14). Like for many apicoplast-hosted pathways, enzymes belonging to the SUF machinery are essentially absent from the mammalian host and as such, they may be seen as good potential drug targets. Noticeably, while most apicoplast proteins are encoded by the parasite nucleus (after gene transfer from the endosymbiont), SUFB is one of the very few proteins still encoded by the apicoplast genome, perhaps illustrating the importance of the pathway for the parasite. This has sparked considerable interest for the SUF pathway in *Plasmodium*, which has been shown to be important for the viability of several developmental stages of the parasite (15–19).

To better understand the contribution of the SUF pathway to *T. gondii* viability, we have generated a conditional mutant for the scaffold protein TgSUFC and conducted a thorough phenotypic characterization of this mutant, together with the TgNFS2 mutant we have previously generated (14). Our results confirm that inactivating the plastid-hosted SUF pathway in *T. gondii* leads to irreversible and marked effects on membrane homeostasis, impacting the division process and parasite viability. We show that these effects are likely due to impairment in the function of several key plastidic Fe-S proteins, which have pleiotropic downstream metabolic consequences for the parasite.

Results

A Toxoplasma *SUFC homolog in the apicoplast*

Searching for homologs of the plant SUF system in the ToxoDB.org database, we have previously shown an overall good conservation for the plastidic Fe-S cluster synthesis pathway (14). Among the candidates for members of the SUF machinery, we have identified a potential *T. gondii* homolog of SUFC, member of a Fe-S cluster scaffold complex comprising SUFC, SUFB, and SUFD (Fig. 1*A*). This complex is also present in prokaryotes, where it was first characterized (20): it was shown that bacterial SufC is an ABC-like ATPase component essential for proper Fe-S cluster assembly (21). Alignment of the amino acid sequences of the *T. gondii* SUFC candidate (entry TGGT1_225800 in the ToxoDB.org database (22)) and its *Escherichia coli* counterpart showed a good overall conservation (56% of identity), particularly in the motifs that are characteristic of ABC ATPAses (Fig. 1*B*). The *T. gondii* protein presents an N-terminal extension when compared with *E. coli* SufC, which may contain a transit peptide for targeting to the apicoplast. Accordingly, it was predicted with high probability to be a plastid-localized protein by the Deeploc 1.0 (https://services.healthtech.dtu.dk/service.php?DeepLoc-1.0) algorithm (23), although the exact position of the N-terminal transit peptide sequence could not be defined. Data from global mapping of *T. gondii* proteins' subcellular location by hyperLOPIT spatial proteomics (24) also suggested an apicoplast localization for TGGT1_225800. To assess whether this protein is a real functional homolog, we first performed complementation assays of an *E. coli* SufC mutant, for which growth is slowed, especially when limiting iron availability with a specific chelator (25). We could show that expressing the predicted functional domain of TGGT1_225800 restored bacterial growth (Fig. 1*C*), even in the presence of the iron chelator, confirming this protein (hereafter named TgSUFC) is functional.

In order to detect TgSUFC expression and assess its subcellular localization in the tachyzoite stage (the fast-replicating stage associated with acute toxoplasmosis (2)), we epitope-tagged the native protein. This was performed by inserting a sequence coding for a C-terminal triple hemagglutinin (HA) epitope tag at the endogenous TgSUFC locus by homologous recombination (Fig. S1). It was achieved in the tetracycline-inducible transactivator (TATi) ΔKu80 cell line, favoring homologous recombination and allowing transactivation of a Tet operator-modified promoter that we subsequently used for generating a conditional mutant in this background (26–28). Immunoblot analysis with an anti-HA antibody revealed two products, likely corresponding to the immature and mature forms (resulting from the cleavage of the transit peptide upon import into the organelle) of TgSUFC (Fig. 2*A*). Immunofluorescence assay (IFA) with the anti-HA antibody and costaining with an apicoplast marker confirmed that TgSUFC localizes to this organelle in *T. gondii* tachyzoites (Fig. 2*B*).

Depletion of TgSUFC blocks parasite growth

Next, we generated a conditional TgSUFC mutant cell line in the TgSUFC-HA–expressing TATi ΔKu80 background. Replacement of the endogenous promoter by an inducible-Tet07SAG4 promoter was achieved through a single homologous recombination at the locus of interest, yielding the conditional knockdown (cKD) TgSUFC-HA cell line (Fig. S2). In this cell line, the addition of anhydrotetracycline (ATc) can repress transcription through a Tet-Off system (29). Initial phenotypic characterization was performed on two independent clones, which were found to behave similarly and thus only one was analyzed further. It should be noted that the promoter replacement resulted in a slightly higher expression of TgSUFC but did not change the maturation profile of the

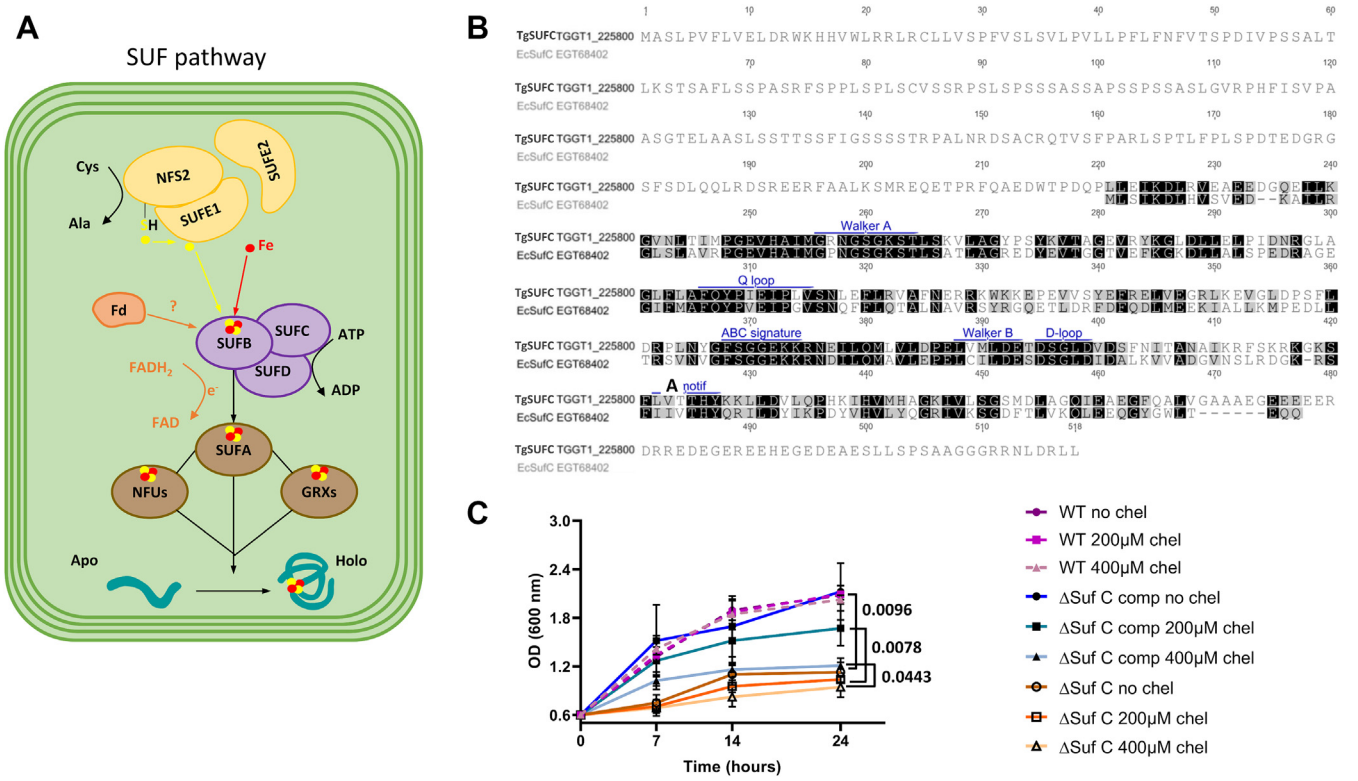

Figure 1. The *Toxoplasma gondii* functional homolog of SufC. *A*, schematic representation of the molecular machinery for Fe-S cluster synthesis in the apicoplast of *T. gondii* (see main text for details). *B*, alignment of the predicted amino acid sequence of TgSUFC and its homolog from *Escherichia coli*. Motifs that are potentially important for ATPase activity are outlined in *blue*. *C*, functional complementation of bacterial mutants for SufC. Growth of WT *E. coli* K12 parental strain, the SufC mutant strain and the mutant strain complemented ('comp') by the *T. gondii* homolog, was assessed by monitoring the optical density at 600 nm in the presence or not of an iron chelator (2,2'-bipyridyl, 'chel'). Values are mean from $n = 3$ independent experiments ±SD. Two-tailed Student's *t* test *p*-values are indicated, when comparing values obtained with various concentrations of chelator for the mutant cell line *versus* the complemented one.

protein (Fig. 2*A*). Downregulation of TgSUFC was assessed by growing the parasites in the presence of ATc. Immunoblot and IFA analyses showed a decrease of TgSUFC to almost undetectable levels after as early as 1 day of ATc treatment (Fig. 2, *A* and *B*). We also generated a complemented cell line constitutively expressing an additional TY-tagged (30) copy of TgSUFC from the uracil phosphoribosyltransferase (UPRT) locus, driven by a tubulin promoter (Fig. S3). This cell line, named cKD TgSUFC-HA comp, was found by immunoblot (Fig. 2*C*) and IFA (Fig. 2*D*) to be stably expressing TgSUFC while the HA-tagged copy was efficiently downregulated in the presence of ATc.

We first evaluated the consequences of TgSUFC depletion on parasite fitness *in vitro* by performing a plaque assay, which determines the capacity of the mutant and complemented parasites to produce lysis plaques on a host cells' monolayer in the absence or continuous presence of ATc for 7 days (Fig. 3). Depletion of TgSUFC prevented plaque formation, which was restored in the complemented cell lines (Fig. 3, *A* and *B*). Our previous analysis of another SUF pathway mutant (TgNFS2, (14)) suggested that the impact on the pathway leads to irreversible death of the parasites, so we sought to verify this by removing the ATc after 7 days of incubation and monitoring plaque formation. We confirmed that depleting TgSUFC was irreversibly impacting parasite viability, as ATc removal did not lead to the appearance of plaques (Fig. 3*C*). We next assessed whether this defect in the lytic cycle is due to a replication problem. Mutant and control cell lines were pre-incubated in the absence or presence of ATc for 48 h and released mechanically, before infecting new host cells and were then grown for an additional 24 h in ATc prior to parasite counting. We noted that the incubation with ATc led to an accumulation of vacuoles with fewer TgSUFC mutant parasites, but that it was not the case in the complemented cell lines (Fig. 3*D*). Overall, our data show that depleting TgSUFC has an irreversible impact on parasite growth, as previously described for other SUF mutant TgNFS2 (14).

SUF pathway mutants display important membrane defects during cell division

T. gondii tachyzoites divide by a process called endodyogeny, whereby two daughter cells will assemble inside a mother cell (31). Among the structures which are essential as a scaffold for daughter cell formation is the inner membrane complex (IMC), a system of flattened vesicles underlying the plasma membrane and is supported by a cytoskeletal network. The IMC also supports anchorage for the glideosome, the protein complex–powering parasite motility (32). As for several other cellular structures, there is a combination of de novo assembly and recycling of maternal material during IMC formation in daughter cells (33). To get more precise insights

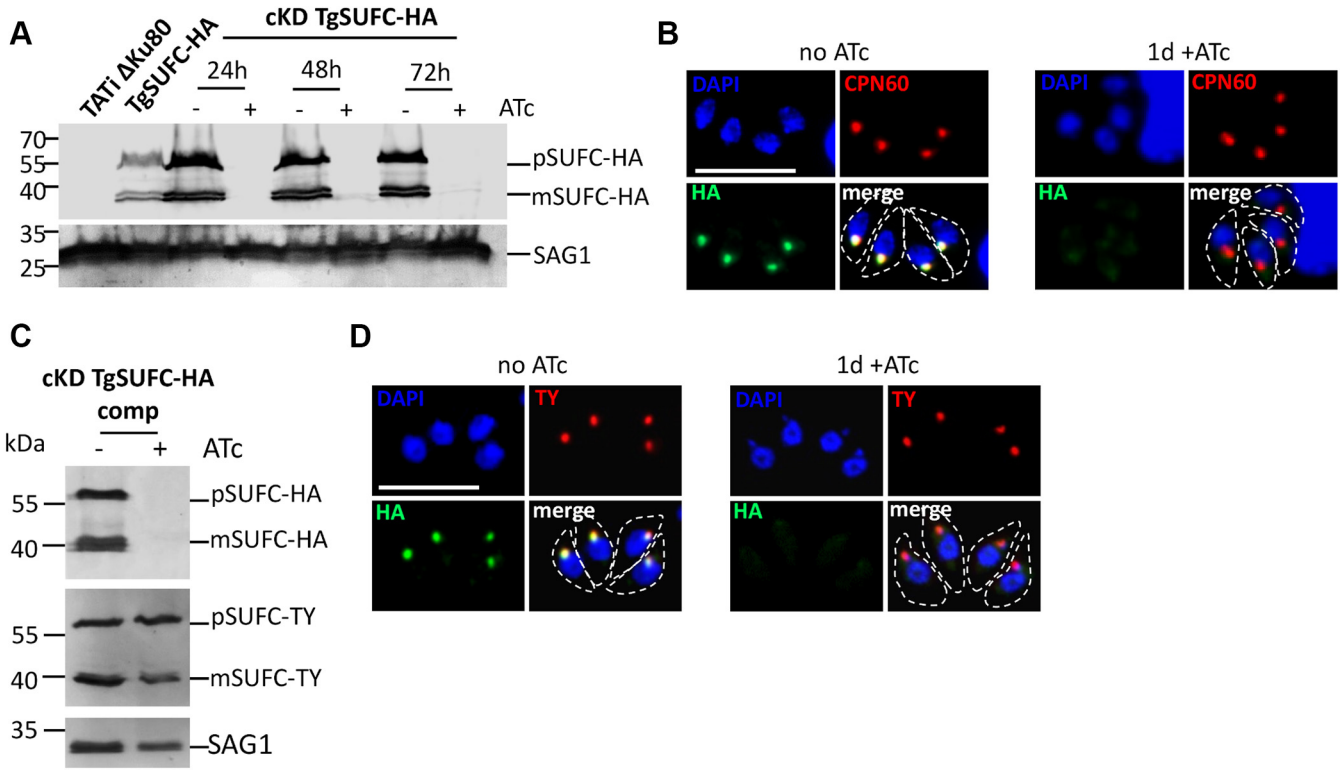

Figure 2. Generation of conditional knockdown and complemented cell lines for the apicoplast-localized TgSUFC. *A*, immunoblot analysis with anti-HA antibody shows precursor (p) and mature (m) forms of C-terminally HA-tagged TgSUFC and efficient downregulation of the protein after 24 h of incubation with ATc. Anti-SAG1 antibody was used as a loading control. *B*, HA-tagged TgSUFC (*green*) localizes to the apicoplast (labeled with marker TgCPN60, *red*) and is efficiently downregulated upon addition of ATc for 24 h. The scale bar represents 5 μm. DNA was labeled with DAPI. Parasite shape is outlined. *C*, immunoblot analysis of the conditional TgSUFC knockdown cell line expressing a TY-tagged version of the protein shows similar processing profile and stable expression after 48 h of ATc addition. *D*, immunofluorescence assay confirms colocalization of the regulatable HA-tagged TgSUFC (*green*) and the TY-tagged additional copy (*red*), whose expression is retained after 24 h of incubation with ATc. The scale bar represents 5 μm. DNA was labeled with DAPI. Parasite shape is outlined. ATc, anhydrotetracycline; DAPI, 4,6-diamidino-2-phenylindole; HA, hemagglutinin; SAG, surface antigen.

into the impact of the impairment of the SUF pathway on parasite division, we incubated the TgNFS2 and TgSUFC mutant parasites with ATc for up to 2 days and stained them for IMC protein IMC3 to detect growing daughter cells (Fig. 4*A*). IMC3 is an early marker of daughter cell budding (34), which is usually synchronized within the same vacuole. However, after 2 days of ATc treatment, an increasing portion of the vacuoles showed a lack of synchronicity for daughter cell budding for both mutant cell lines, although the effect was more pronounced for the TgSUFC mutant (Fig. 4, *A* and *B*).

Then, we used electron microscopy to get a subcellular view of the consequences of TgNFS2 and TgSUFC depletion on the cell division process. Strikingly, in parasites grown in the continuous presence of ATc for 3 days, we observed cytokinesis completion defects. As budding daughter cells emerge, they normally incorporate plasma membrane material that is partly recycled from the mother, leaving only a basal residual body. Here, in both TgNFS2 and TgSUFC mutant cell lines, daughter cells remained tethered through patches of plasma membrane (Fig. 4*C*). Hence, this highlighted an early and important defect in plasma membrane biogenesis and/or recycling during daughter cell budding. We previously observed major cell division defects after long term (5 days or more) continuous incubation of cKD TgNFS2-HA parasites with ATc (14). When assessing the cKD TgSUFC-HA parasites in the same conditions, costaining with apicoplast and IMC markers revealed similar defects, including organelle segregation problems and abnormal membranous structures (Fig. 4*D*).

Depletion of TgSUFC has an impact on the apicoplast

Computational prediction of the Fe-S proteome combined with hyperLOPIT localization data suggests there are a limited number of apicoplast proteins potentially containing Fe-S clusters (14). However, these candidates are supposedly very important for the parasite. They include the following: IspG and IspH, two oxidoreductases involved in isoprenoid synthesis (35); LipA, a lipoyl synthase important for the function of the pyruvate dehydrogenase (PDH) complex (36); MiaB, which is likely a tRNA modification enzyme (37); as well as proteins that are directly involved in Fe-S synthesis, and the plastidic ferredoxin (Fd) that is an important electron donor that regulates several apicoplast-localized pathways (38–40). Dataset from a CRISPR-based genome-wide screen suggests that most of these candidates are important for fitness *in vitro* (41).

We first assessed whether depletion of TgSUFC led to a partial apicoplast loss, as was previously shown for TgNFS2 (14). Although slowed down in growth, some parasites eventually egressed during the course of the experiments and were used to reinvade host cells and were kept for a total of 5 days in the presence of ATc (Fig. 5*A*). This is reminiscent to the so-called "delayed death" effect, observed when inhibiting

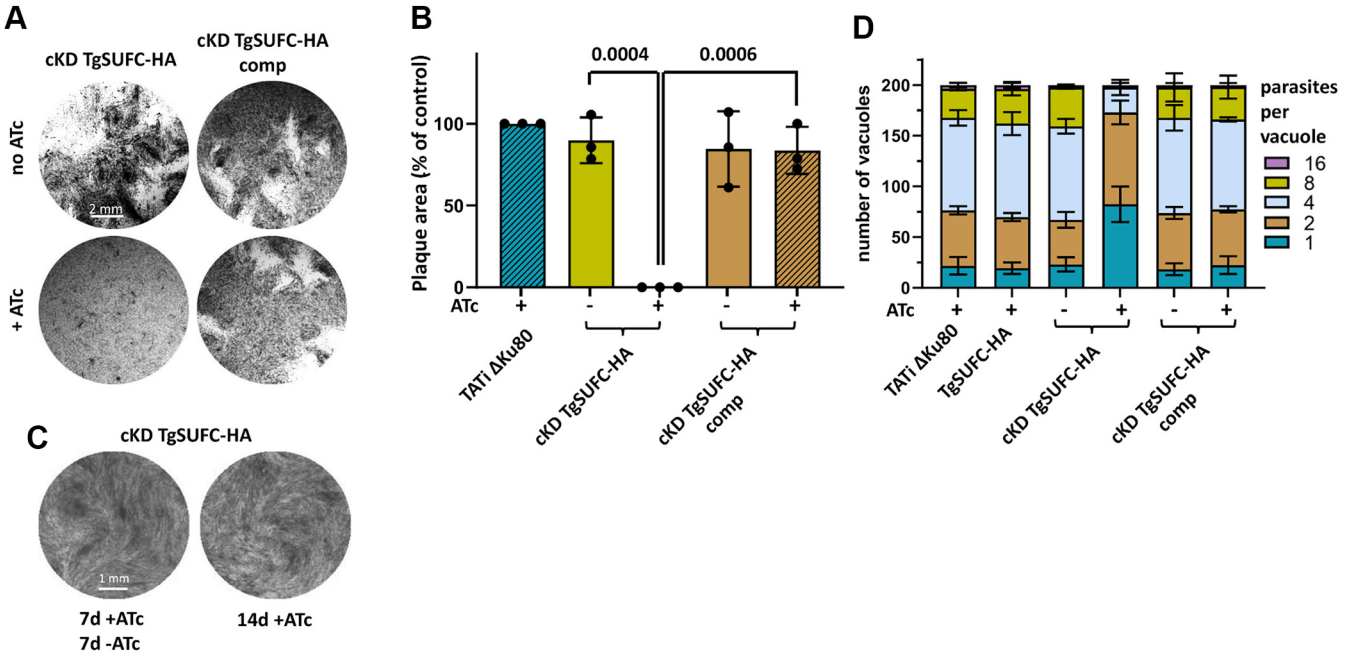

Figure 3. Depletion of TgSUFC affects *in vitro* growth of the tachyzoites irreversibly. *A*, plaque assays were carried out by infecting HFF monolayers with the TgSUFC2-HA conditional knockdown and complemented cell lines. They were grown for 7 days ± ATc. *B*, measurements of lysis plaque areas highlight a significant defect in the lytic cycle when TgSUFC is depleted. Values are means of $n = 3$ experiments ±SD. Mean value of a TATi ΔKu80 control grown in the presence of ATc (not shown on the *left*) was set to 100% as a reference. Two-tailed Student's *t* test *p*-values are indicated. The scale bar represents 2 mm. *C*, plaque assays for the TgSUFC mutant was performed as described in (*A*), but ATc was washed out after 7 days (7days+ATc 7days-ATc) or not (14days+ATc), and parasites were left to grow for an extra 7 days. No plaque was observed upon ATc removal. Shown are images from one representative out of three independent experiments. The scale bar represents 1 mm. *D*, TgSUFC mutant and complemented cell lines, as well as their parental cell line and the TATi ΔKu80 control, were grown in HFF in the presence or absence of ATc for 48 h and subsequently allowed to invade and grow in new HFF cells for an extra 24 h in the presence of ATc. Parasites per vacuole were then counted. Values are means ±SD from $n = 3$ independent experiments for which 200 vacuoles were counted for each condition. ATc, anhydrotetracycline; HA, hemagglutinin; TATi, tetracycline-inducible transactivator.

apicoplast metabolism, that often results in slow-kill kinetics (8). Quantification of the apicoplast marker TgCPN60 showed a progressive loss of this protein (Fig. 5, *A* and *B*). As this could reflect a specific impact on this protein marker rather than a general loss of the organelle, we also stained the parasites with fluorescent streptavidin (mainly detects the biotinylated apicoplast protein acetyl-CoA carboxylase (42)), confirming a similar loss of signal after 5 days of incubation with ATc (Fig. S4). This suggests TgSUFC depletion leads to a progressive but late and partial loss of the apicoplast. Of note, this effect on the organelle is less marked than when TgNFS2 was depleted (14).

One of the apicoplast-localized Fe-S proteins whose activity can be assessed is LipA, which is responsible for the lipoylation of a single apicoplast target protein, the E2 subunit of the PDH (43). We performed an immunoblot analysis with an anti-lipoic acid antibody on protein extracts from cKD TgSUFC-HA parasites kept in the presence of ATc for up to 4 days (Fig. 5, *C* and *D*). We noticed a progressive decrease in lipoylated PDH-E2 to almost no signal after 3 days of ATc incubation. Using an antibody that we specifically raised against the E2 subunit of the PDH (Fig. S5), we verified this was not due to a decrease in global levels of this particular protein. Overall, this is comparable to what we previously described upon depletion of TgNFS2 (14). Thus, disrupting the SUF pathway has direct consequences on Fe-S protein–dependent metabolic pathways hosted by the apicoplast, and prolonged depletion of SUF proteins can even lead to partial loss of the organelle.

Impact of SUF pathway disruption on FA metabolism

The PDH complex generates acetyl-CoA, which is the first step needed to fuel the FASII system in the apicoplast. This pathway generates FA precursors that can be subsequently elongated in the endoplasmic reticulum and are major components of cellular lipids (44, 45). These *de novo*–synthesized FA from the apicoplast FASII can be used as essential building blocks, in combination with scavenged host FA, for bulk phospholipid synthesis allowing essential parasite membrane biogenesis (46, 47). We thus first wanted to evaluate the impact of the perturbation of the SUF pathway on the parasite's FA content and homeostasis. Total FA abundance from the TgNFS2 and TgSUFC mutant cell lines were determined and quantified by GC-MS–based analyses. Interestingly, for the TgNFS2 and TgSUFC mutants, there was a significant decrease in the abundance of shorter FAs like C14:0, which is typically synthesized by the FASII system in the apicoplast (Fig. 6, *A* and *B*). This suggests that de novo FA synthesis could be affected in these mutants.

While FASII was shown previously to be critical for tachyzoite fitness (43), recent investigations have shown that tachyzoites are capable to sense and adapt their lipid synthetic/acquisition capacities according to the host nutrient content and/or lipid availability. For instance, they are able to upregulate their FASII activity if nutrients are scarce in the host or to downregulate it if scavenged lipid levels are too high (47). Moreover, scavenging FA precursors from their host cells allows tachyzoites to at least partly compensate for a lack of *de*

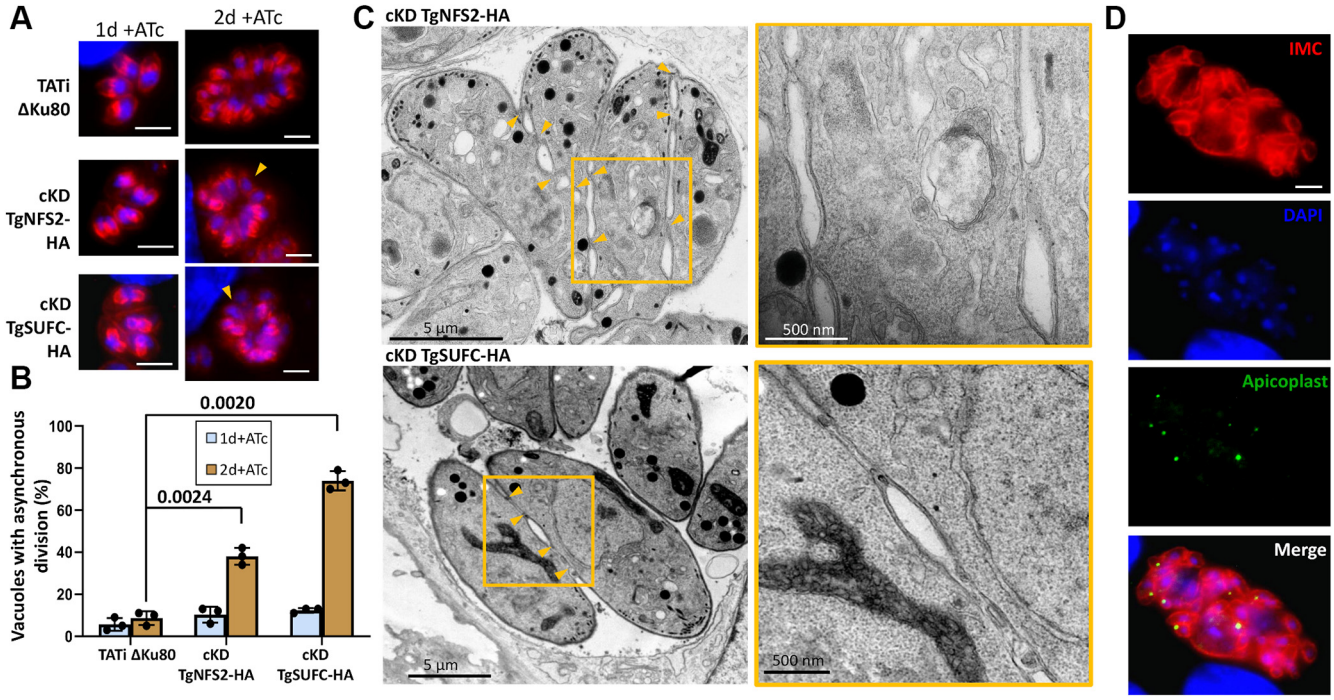

Figure 4. Depletion of TgNFS2 or TgSUFC leads to membrane defects during cell division. *A*, TgNFS2-HA and TgSUFC-HA conditional knockdown parasites as well as a TATi ΔKu80 control were grown in the presence of ATc for up to 2 days and were stained with an anti-TgIMC3 antibody (in *red*, to outline parasites and internal buds - *top*). In a normal situation, internal budding of parasites is generally synchronous within the same vacuole. Upon depletion of TgNFS2 or TgSUFC, dividing and nondividing parasites are occasionally present together within the same vacuole (*arrowheads*). The scale bar represents 5 µm. DNA was labeled with DAPI (*blue*). *B*, the percentage of vacuoles presenting asynchronous division as illustrated in (*A*) has been quantified and is represented as a means of $n = 3$ experiments ±SD (*bottom*). Two-tailed Student's *t* test *p*-values are indicated. *C*, electron microscopy analysis of TgNFS2-HA and TgSUFC-HA conditional mutants grown for 4 days in the presence of ATc shows default in plasma membrane separation during parasite division, as displayed on insets representing magnifications of selected parts of the respective *left image*. *D*, cKD TgSUFC-HA parasites that were grown in the presence of ATc for 5 days were costained with anti-TgIMC3 to outline the inner membrane complex and anti-TgCPN60 (an apicoplast marker), which highlighted abnormal membrane structures and organelle segregation problems. The scale bar represents 5 µm. DNA was labeled with DAPI. ATc, anhydrotetracycline; cKD, conditional knockdown; DAPI, 4,6-diamidino-2-phenylindole; HA, hemagglutinin; IMC, inner membrane complex; TATi, tetracycline-inducible transactivator.

novo synthesis (46, 48). Thus, to investigate whether the SUF mutants have their lipid synthesis/flux affected, we sought to assess the impact of TgNFS2 and TgSUFC depletion on de novo–synthesized *versus* scavenged FAs by stable isotope precursor labeling with ^{13}C glucose combined with mass spectrometry–based analyses (45–47). The analyses revealed a significant increase in the levels of host-scavenged FAs upon the disruption of TgSUFC (Fig. 6*D*). This was not observed in the complemented cell line (Fig. S6) and thus most likely reflects a mechanism for compensating the lack of de novo–made FAs by increasing scavenging host-derived FAs. On the other hand, this was not as obvious for the TgNFS2 mutant (Fig. 6*C*).

The ability of tachyzoites to survive lack of de novo lipid synthesis is highly dependent on the availability of exogenous lipid precursors. Others have shown that FASII mutants could be rescued by the addition of palmitic (C16:0) or myristic (C14:0) acid for instance (44, 48, 49). We thus tried to compensate the impact of TgNFS2 and TgSUFC depletion on the parasite lipid homeostasis by supplementing the growth medium with these FAs and performing plaque assays. Palmitic acid supplementation partially restored growth of the TgNFS2 mutant (Fig. 7, *A* and *B*), while with myristic acid, only after long term incubation (up to 2 weeks) these mutant parasites started growing back (Fig. 7, *C* and *D*). In contrast, depletion of TgSUFC was not efficiently compensated by exogenous fatty supplementation (Fig. 7). Based on our flux analysis, depletion of TgNFS2 affects the levels of short de novo FA content but mutant parasites are not capable to scavenge more FA from the host membrane lipids (Fig. 6, *A* and *C*), it is thus possible that providing excess of free FA may help to compensate for this lack of FA and eventually improve fitness of the mutant parasites. On the other hand, TgSUFC mutant parasites do scavenge significantly more FA from the host already (Fig. 6*F*), and medium supplementation with more exogenous FAs does not seem to further improve their fitness.

This highlights differences between the two SUF pathway mutants with regards to adaptation to the perturbation of lipid homeostasis, which may be explained by different kinetics in depletion of the respective proteins or a different impact on global apicoplast function. In any case, our data confirm that apicoplast-based FA production is affected in SUF pathway mutants, and while these parasites establish compensatory mechanisms by scavenging exogenous lipid precursors, they do not allow them recovering to full fitness. This suggests that perturbation of apicoplast FA synthesis is not the only, and likely not even the primary, effect of SUF pathway disruption impacting parasite growth.

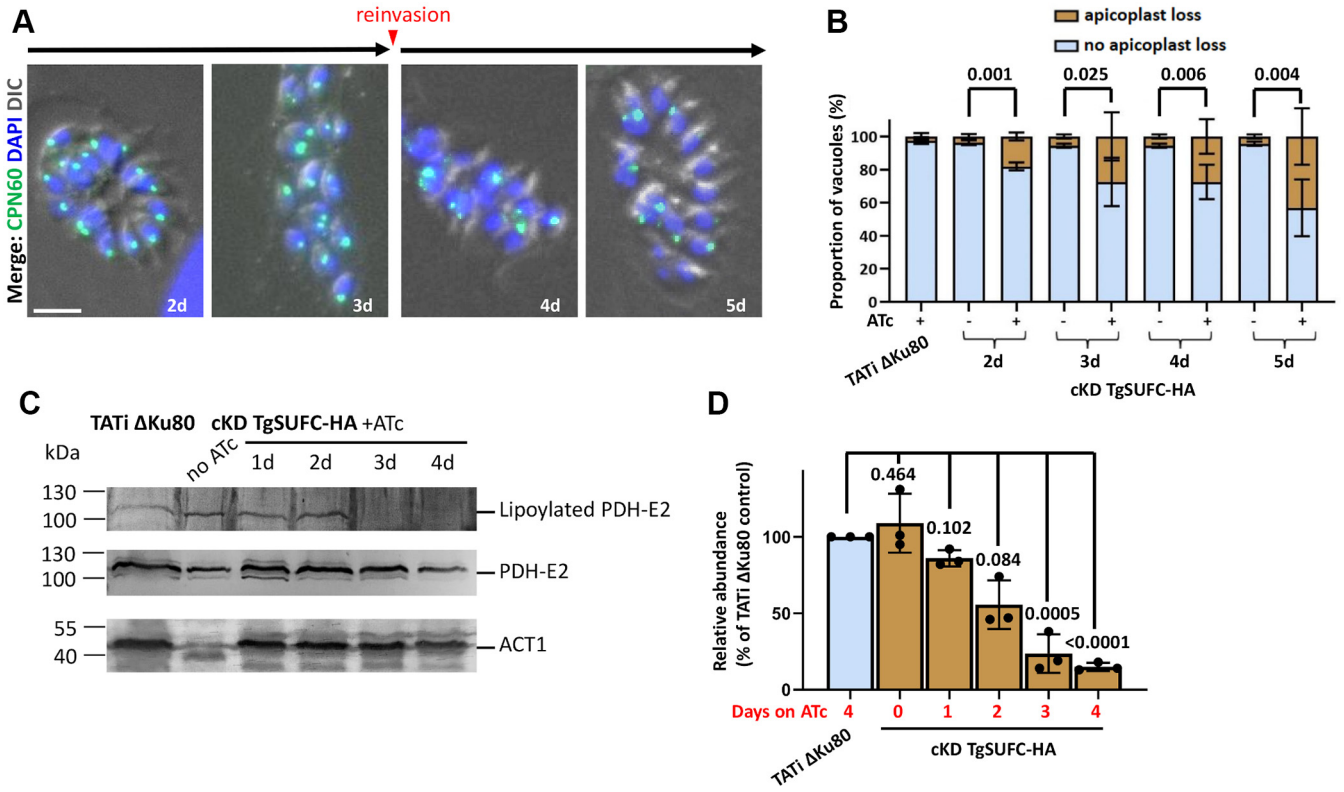

Figure 5. TgSUFC depletion impacts apicoplast-hosted Fe-S pathways. *A*, cKD TgSUFC-HA parasites were kept in the presence of ATc for up to 5 days, and the aspect of the apicoplast was evaluated by microscopic observation using the specific CPN60 marker. After 3 days, parasites egressed and were used to reinvade new host cells for subsequent timepoints. The scale bar represents 5 μm. DNA was labeled with DAPI. *B*, using the labeling described in (*A*), apicoplast loss in vacuoles was monitored after 2 to 5 days of incubation with ATc. At least 50 vacuoles were assessed per condition, and the percentage of vacuoles presenting less apicoplasts than the total number of parasites was recorded (reflecting at least a partial apicoplast loss within the vacuole). Data are mean values from $n = 3$ independent experiments ±SD. Two-tailed Student's *t* test *p*-values are indicated. *C*, a decrease in the lipoylation of the E2 subunit of pyruvate dehydrogenase (TgPDH-E2), which depends on the apicoplast-hosted Fe-S–containing lipoyl synthase LipA, was observed by immunoblot using an antilipoic acid antibody on cell extracts from cKD TgSUFC-HA parasites kept with ATc for an increasing period of time. A polyclonal antibody raised against PDH-E2 was used as a control for global abundance of the protein and for apicoplast integrity. TgACT1 was used as a loading control. *D*, decrease of lipoylated TgPDH-E2 was quantified by band densitometry and normalized with the internal loading control. Data represented are mean ±SD of $n = 3$ independent experiments. Two-tailed Student's *t* test *p*-values are indicated. DIC, differential interference contrast; Fe-S, iron-sulfur; HA, hemagglutinin; ATc, anhydrotetracycline; PDH, pyruvate dehydrogenase; DAPI, 4,6-diamidino-2-phenylindole; cKD, conditional knockdown; LipA, lipoyl synthase.

SUF pathway disruption also has an impact on isoprenoid-dependent pathways

The other main apicoplast-localized biosynthetic pathway potentially affected by disruption of the SUF machinery is isoprenoid synthesis, through the two Fe-S–containing proteins IspG and IspH that are needed for the synthesis of the five carbon precursor isopentenyl pyrophosphate (IPP) and its isomer dimethylallyl pyrophosphate (35). Synthesis of these isoprenoid building blocks is the only essential metabolic function of the apicoplast in the asexual intraerythrocytic stages of *Plasmodium*, where the loss of the organelle can be simply compensated by supplementation with exogenous IPP (50). *Plasmodium* SUF mutants survive when cultured in the presence of IPP, confirming the essential role of the Fe-S synthesizing pathway in this parasite is likely for isoprenoid synthesis (15). Isoprenoid synthesis is also vital for *T. gondii* tachyzoites (51); however, IPP supplementation to the culture medium is not possible probably because, unlike for *Plasmodium*, the highly charged IPP does not efficiently reach the parasite cytoplasm. Tachyzoites can nevertheless scavenge some isoprenoid precursors from their host cells (52). Apicoplast-derived isoprenoid precursors are mostly known for their involvement in important posttranslational protein modifications like prenylation, glycosylphosphatidylinositol (GPI) anchoring, as well glycosylation, in addition to the synthesis of quinones and several antioxidant molecules (35).

In *Plasmodium*, it is believed that prenylated proteins that regulate vesicle trafficking are key in the delayed death phenotype caused by apicoplast loss (53). As geranylgeraniol (GGOH), an isoprenoid precursor for protein farnesylation/prenylation, was successfully used to at least partially complement deficiencies in apicoplast isoprenoid production (52, 54), we tried to supplement the culture medium with GGOH and perform plaque assays with the SUF mutants we generated. However, we did not detect any restoration of growth (Fig. S7*A*). In contrast to *Plasmodium* (55, 56), the prenylome of *T. gondii* is still largely uncharacterized, but using an anti-farnesyl antibody, we did not detect obvious alterations in the general profile of prenylated proteins upon depletion of TgNFS2 or TgSUFC (Fig. S7*B*). Although apicoplast-generated IPP and dimethylallyl pyrophosphate are also necessary for synthesizing the farnesyl diphosphate used for protein prenylation in *T. gondii* tachyzoites, it is thus possible that these parasites can initially scavenge host-derived isoprenoids to

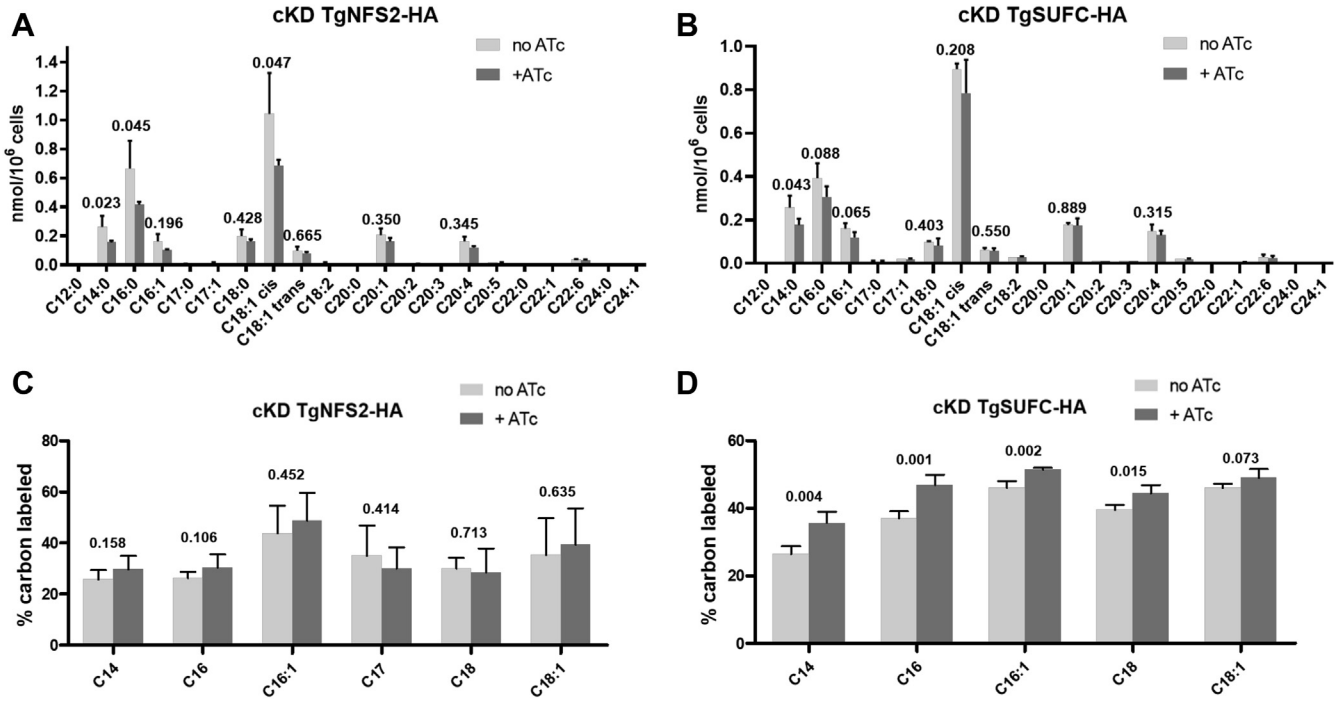

Figure 6. Total content and flux analyses upon TgNFS2 and TgSUFC depletion reveals changes in FA homeostasis and fluxes. Total FA content for the cKD TgNFS2-HA (*A*) and the cCK TgSUFC (*B*) mutants was determined by GC-MS analyses and suggest a decrease in shorter chain FAs like C14:0 upon depletion of SUF proteins by ATc. Host-scavenged FAs were determined by stable isotope labeling combined to GC-MS analyses on the TgNFS2 (*C*) and TgSUFC (*D*) cKD mutants and reveal a significant increase of host lipid scavenging upon TgSUFC depletion by ATc. All data are mean from $n = 4$ (or $n = 3$ for panel *B*) independent experiments ±SD; indicated are two-tailed Student's *t* test *p*-values showing significance of changes in main FA species abundance. ATc, anhydrotetracycline; cKD, conditional knockdown; FA, fatty acid; HA, hemagglutinin.

compensate for a deficient *de novo* production (52). In any case, altogether our results suggest that defects in protein farnesylation/prenylation may not be one of the primary consequences of SUF pathway disruption in *T. gondii*.

We next sought to investigate the potential impact of TgNFS2 or TgSUFC depletion on GPI-anchoring. The surface antigen (SAG)–related sequence family comprising proteins related to SAG1, the first characterized *T. gondii* surface antigen, is arguably the best characterized family of GPI-anchored proteins in the parasite (57). We preincubated mutant parasites for 3 days with ATc and allowed them to invade and grow into host cells for an extra day in the presence of ATc before using specific antibodies to detect GPI-anchored SAG1 and SAG3. We could see obvious signs of mislocalization for these two proteins that, instead of keeping a homogenous peripheral distribution, were often seen accumulated at the apex or base of the parasites, or even found within the parasitophorous vacuole space (Fig. 8, *A* and *B*). Interestingly, while the SAG1 protein appears to be distributed differently by IFA, our previous immunoblot analyses suggest there is no drastic change in the total amount of protein upon TgNFS2 or TgSUFC depletion ((14) and Fig. 2*A*). It was previously shown that the deletion of SAG1's GPI anchor leads to a constitutive secretion of this protein to the parasitophorous vacuole space (58). It should be noted that, in contrast to the distribution of GPI-anchored SAG proteins, in these experimental conditions, the overall structure of the IMC appeared unaffected (Fig. 8*A*). Hence, our data suggest that disruption of the SUF pathway perturbs GPI anchor formation.

Another important posttranslational modification depending on isoprenoid-containing dolichol is glycosylation. Several key proteins of the glideosome complex are supposedly glycosylated and, as a consequence, glycosylation inhibition has been reported to impact parasite motility (59–61). We thus performed gliding motility assays on the SUF mutants. Typically, this is done by monitoring the shedding of SAG1 that leaves trails when tachyzoites glide on solid substrates. Perhaps as a consequence of SUF pathway disruption on SAG1 targeting, trails were clearly less abundant upon depletion of TgNFS2 and TgSUFC (Fig. 8, *C* and *D*). We could nevertheless detect and measure trails, whose mean length provides an estimate of overall motility rates, and they were found to be significantly smaller in the absence of TgNFS2 or TgSUFC (Fig. 8*E*). We sought to further verify the robustness of these results in an SAG1-independent manner. As membranes are shed during gliding, trails are not only rich in surface proteins but also in lipids (62). We thus used a marker of membrane lipids [DiI (1,1′-dioctadecyl-3,3,3′,3′-tetramethylindocarbocyanine), a lipophilic membrane stain] in the same type of assay and confirmed that gliding motility of the SUF mutants is less efficient (Fig. S8). Thus, our results suggest that protein glycosylation is also affected upon disruption of the SUF pathway. Overall, our findings indicate that the depletion of proteins of the SUF pathway leads to defects in the synthesis of isoprenoid precursors with consequences on the post-translational modification and targeting of proteins of the peripheral membrane system.

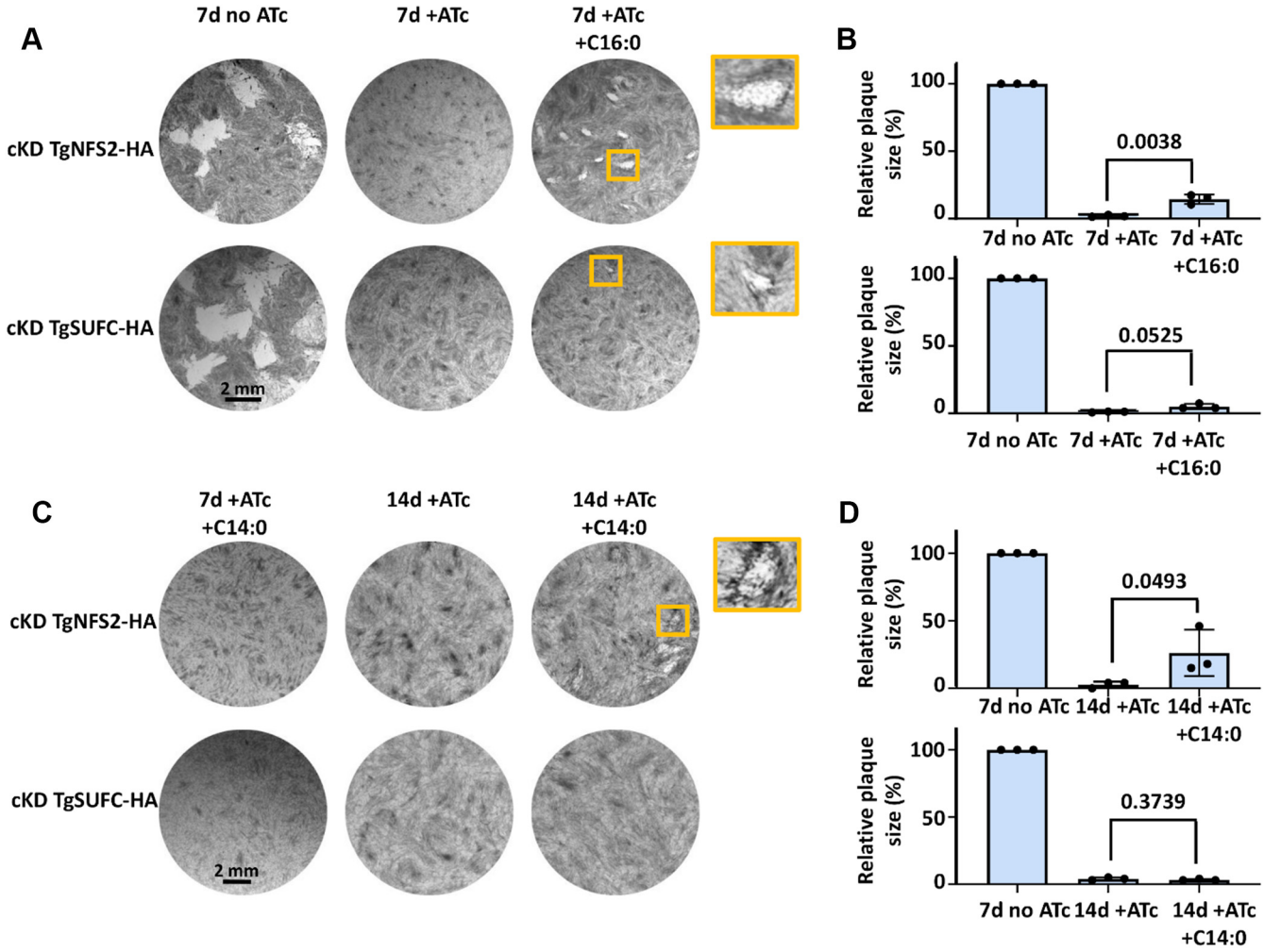

Figure 7. Exogenous supplementation with short chain FAs only partially restore fitness of cKD TgNFS2 and cKD TgSUFC mutant parasites *in vitro*. Plaque assays were performed as described in Figure 3*A*, in the absence or presence of 50 μM of palmitic (C16:0; *A* and *B*) or myristic (C14:0; *C* and *D*) acid. Plaque sizes were measured and area was expressed as a percentage of the value obtained after 7 days of growth in the absence of ATc. All data are mean values from $n = 3$ independent experiments ±SD. Two-tailed Student's *t* test *p*-values are indicated. Palmitic acid allows partial restoration of plaques with the cKD TgNFS2 mutant and to a lesser extent with the cKD TgSUFC mutant after 7 days of growth; myristic acid partially restored plaques but only for the cKD TgNFS2 mutant and after 2 weeks of incubation. ATc, anhydrotetracycline; cKD, conditional knockdown; FA, fatty acid.

Discussion

Beside components of the SUF Fe-S cluster synthesis machinery, the apicoplast harbors only a small number of putative Fe-S proteins (Fig. 9, (14)). Yet, they are all presumably important for parasite fitness as suggested by their negative scores with a CRISPR-based genome-wide screen (Fig. 9, (41)). However, not all are expected to be absolutely essential *in vitro*. The tRNA-modifying enzyme MiaB, for instance, has only a moderately low fitness score and has been shown recently to be dispensable for *Plasmodium* intraerythrocytic stages (40). Similarly, the LipA lipoyl synthase essential for the function of the E2 subunit of the PDH complex, which is in turn crucial for generating the acetyl-CoA necessary for de novo FA synthesis in the apicoplast, seems dispensable for *Plasmodium* blood stages (40), for which the FASII system is not essential in high nutrient-content medium (46, 63). However, given the potentially greater importance of FASII in *T. gondii* tachyzoites (43), this is something we investigated further. We demonstrated that disruption of the SUF pathway–impaired LipA function and PDH-E2 lipoylation (Fig. 5) and, likely as a consequence of this and FASII perturbation, general production of myristic and palmitic acid in the parasites (Fig. 6). However, the growth defect of SUF mutants could only be partially complemented by FA supplementation for the TgNFS2 mutant, and not at all for the TgSUFC mutant (Fig. 7), suggesting perturbation of FASII is not the primary cause of death for these mutants. While it is undoubtedly a metabolic pathway that plays a central role for parasite fitness, the view on the essentiality of FASII in *T. gondii* tachyzoites has recently evolved. There is now published evidence that parasites can adapt their metabolic capacities depending on the nutrient environment (46, 47, 64) and even survive *in vitro* when FASII enzymes are inactivated (48, 65). There is clearly flexibility in the adaptation of parasite pathways to lipid sources (46, 47, 66). As tachyzoites can readily scavenge and incorporate FAs from exogenous sources (i.e., phospholipid made by the host cell and/or phospholipids and FA scavenged from the extracellular medium) into their

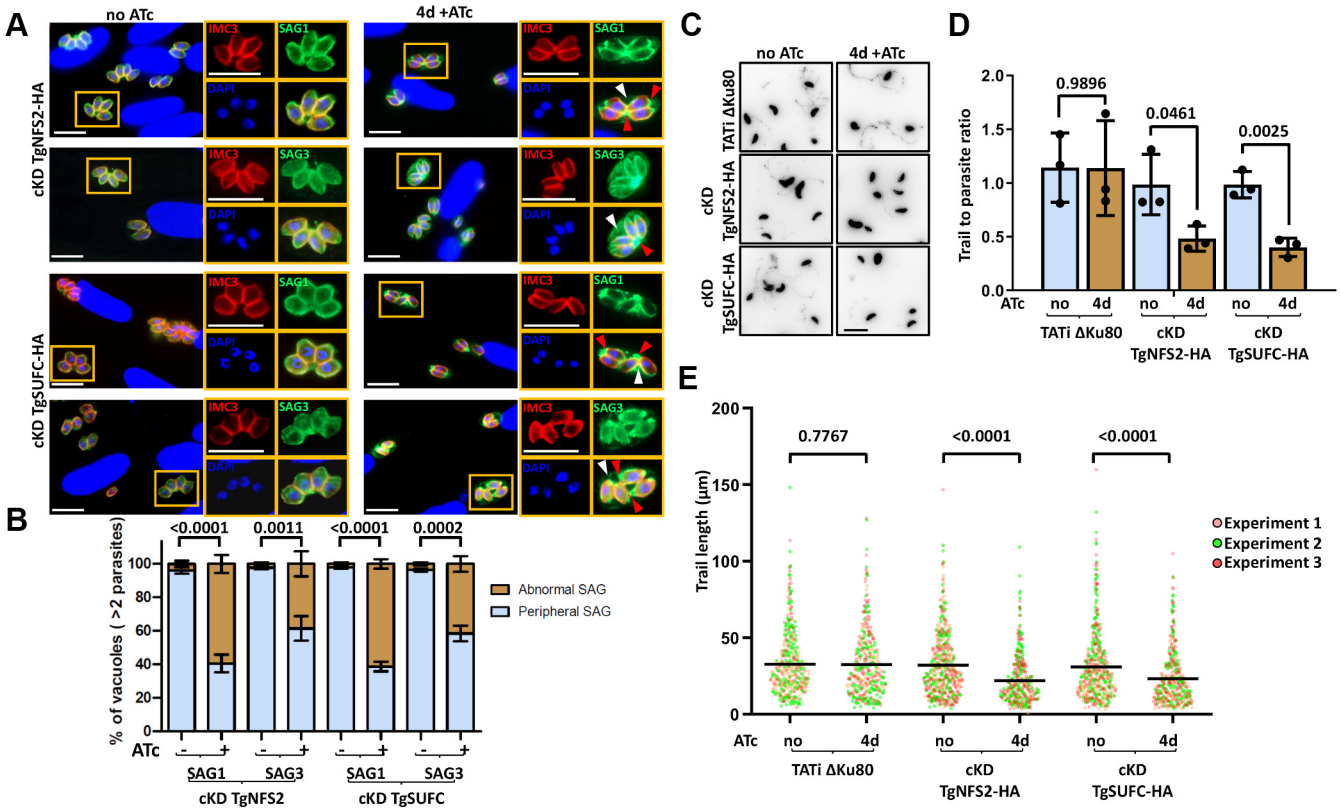

Figure 8. The depletion of TgNFS2 or TgSUFC leads to mislocalization of GPI-anchored surface antigens and impacts gliding motility. *A*, TgNFS2 and TgSUFC conditional mutants were grown for 3 days in the presence or absence of ATc and allowed to invade host cells for another 24 h in the presence or absence of ATc. Parasites were then costained for inner membrane complex marker IMC3 (*red*) together with GPI-anchored protein SAG1 or SAG3 (*green*). As shown on insets representing selected parts of the images, the depletion of TgNFS2 or TgSUFC leads to the accumulation of SAGs in the vacuolar space (*white arrowhead*) or concentration at the apex or base of the parasite (*red arrowhead*). The scale bar represents 10 µm. DNA was labeled with DAPI. *B*, quantification of the abnormal distribution of SAG labeling in vacuoles containing more than two parasites. Data are mean values from $n = 3$ independent experiments ±SD. Two-tailed Student's *t* test *p*-values are indicated. *C*, representative views of a gliding assay showing *lower* abundance of SAG1 trails upon TgNFS2 or TgSUFC depletion (inverted *grayscale* images). The scale bar represents 10 µm. *D*, quantification of the trail to parasite ratio on at least ten randomly selected fields. Data are mean values from $n = 3$ independent experiments ±SD. Two-tailed Student's *t* test *p*-values are indicated. *E*, individual measurements of SAG1 trail lengths. *Horizontal lines* represent mean values from $n = 3$ independent experiments. At least 100 trails were measured for each dataset. Two-tailed Student's *t* test *p*-values are indicated. ATc, anhydrotetracycline; DAPI, 4,6-diamidino-2-phenylindole; GPI, glycosylphosphatidylinositol; IMC, inner membrane complex; SAG, surface antigen.

own range of lipids (46–48, 67), in the end the essentiality of the FASII pathway depends largely on nutrient availability *in vivo* or *in vitro* through culture conditions provided (64).

The other main metabolic pathway that depends directly on Fe-S proteins in the apicoplast is for the synthesis of isoprenoid precursors. When their isoprenoid production is inhibited, *T. gondii* tachyzoites can scavenge some of these precursors from the host cell, leading to a delayed death effect (52, 68), but that cannot fully compensate for a lack of de novo synthesis. Isoprenoids are a large and diverse class of lipids whose cellular functions in Apicomplexa still remain to be extensively characterized, but they include synthesis of vitamins and cofactors (ubiquinone), and are also involved in important post-translational modifications of proteins, like prenylation, GPI-anchoring, and glycosylation (Fig. 9, (35)). Ubiquinone is a central molecule in the mitochondrial electron transport chain (ETC): its quinone head is the functional group for the transfer of electrons, whereas the isoprenoid tail primarily serves for anchoring to the inner mitochondrial membrane. The mitochondrial ETC is a validated drug target in Apicomplexa, for which complex III inhibitor atovaquone has been used in therapeutic strategies (69). However, while *T. gondii* mitochondrial ETC mutants are severely impaired in growth (70–73), it seems that genetic or pharmaceutical inactivation of the ETC (with atovaquone for instance) is reversible (14, 72) and may lead to stage conversion into a metabolic dormant state rather than complete death of the parasites. On the contrary, the viability of the SUF mutants is irreversibly affected (Fig. 3*C* and (14)). So, although the impact SUF protein depletion on the isoprenoid pathway is likely to lead to a deficiency in ubiquinone synthesis, which in turn would contribute to a decrease in parasite fitness, this is probably not the main reason for the irreversible death of the parasites.

In *Plasmodium* blood stages, where isoprenoid synthesis is the only essential pathway hosted by the apicoplast, disrupting the prenylation of Rab GTPAses, which are involved in vesicular trafficking, contributes to delayed death (53). In *T. gondii*, interestingly, perturbation of Rab function can lead to intracellular accumulation and patchy surface distribution of SAG1 proteins and results in defects in the delivery of new membrane required for completing daughter cell segregation at the end of cytokinesis (74, 75). This bears some similarity

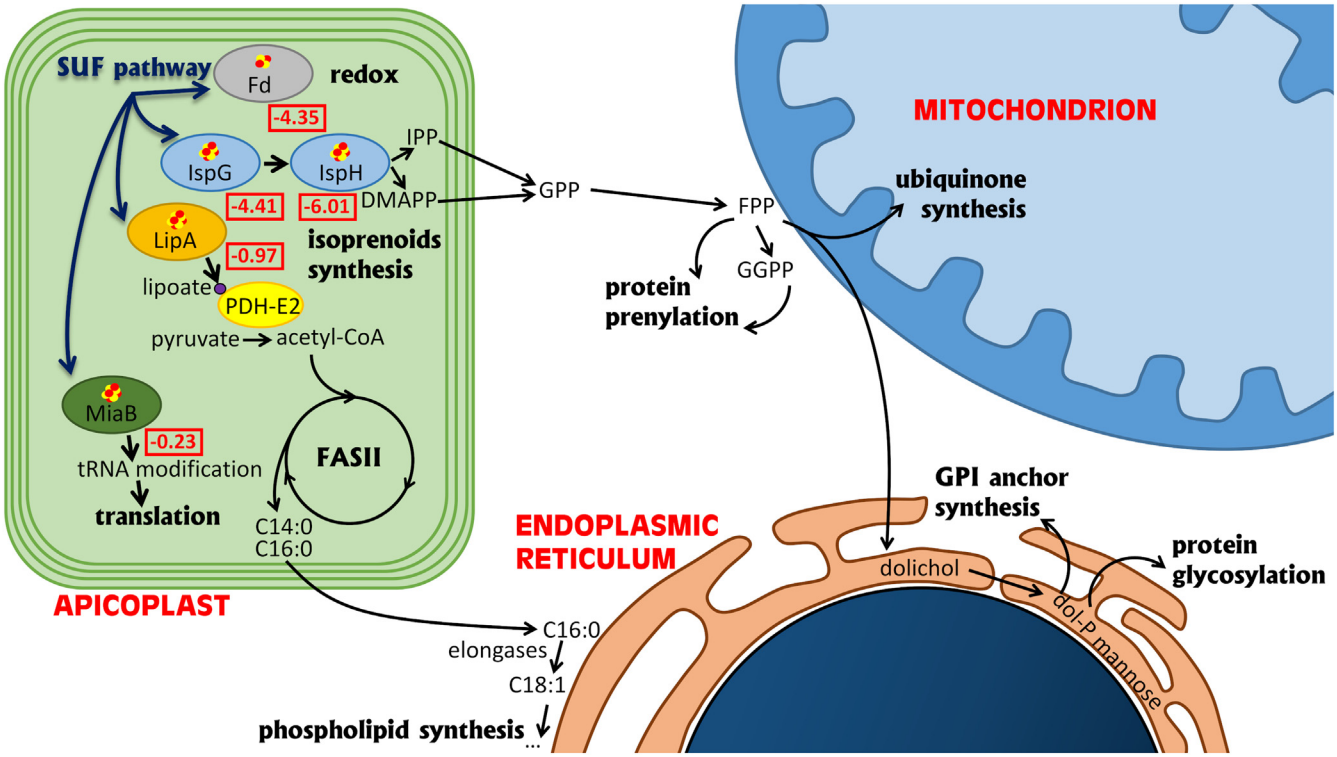

Figure 9. Schematic representation of the main cellular pathways that depend on apicoplast Fe-S proteins. For selected apicoplast-located Fe-S proteins, *squared red* numbers represent CRISPR fitness score of the corresponding gene (genes that contribute to *in vitro* parasite fitness are represented by negative scores; values below −2.5 highlight increasing likelihood of being essential). CoA, coenzyme A; dol-P, dolichol phosphate; DMAPP, dimethylallyl diphosphate; FASII, fatty acid synthesis type II; Fd, ferredoxin; Fe-S, iron-sulfur; FPP, farnesyl diphosphate; GPP, geranyl diphosphate; GGPP, geranylgeranyl diphosphate; GPI, glycosylphosphatidylinositol; IPP, isopentenyl diphosphate; IspG/IspH, oxidoreductases catalyzing the last two steps of IPP/DMAPP synthesis; LipA, lipoyl synthase; PDH-E2, E2 subunit of the pyruvate dehydrogenase complex.

with some phenotypes we have observed in the SUF mutants; yet, while we cannot completely exclude Rab prenylation is perturbed in the SUF mutants, we did not identify any particular prenylation problem in the parasites, and we failed to complement their growth defect with prenylation precursor GGOH (Fig. S7). We thus investigated other important isoprenoid-dependent protein modifications. For instance, upon sugar addition, dolichol can be used for the formation of GPI anchors or act as a donor for protein glycosylation. Our phenotypic analysis revealed that the targeting of GPI-anchored surface proteins and the gliding motility of the parasites, which relies on glycosylated proteins, were clearly affected upon disruption of the SUF pathway (Fig. 8). This confirms the importance of the apicoplast Fe-S cluster synthesis machinery for isoprenoid metabolism. In *Plasmodium*, interfering with apicoplast-hosted isoprenoid production affects the morphology of the organelle (76), but depletion of IspG and IspH does not lead to loss of the apicoplast (40), while interfering with the SUF pathway does (15). We also observe a late impact on the organelle (Fig. 5) that suggests the long term phenotypic consequences of SUF proteins in *T. gondii* are indeed multifactorial and would extend beyond the simple disruption of the isoprenoid pathway.

At the cellular level, one of the most visible consequence of long term depletion of SUF proteins is the membrane defects in the late stages of cytokinesis (Fig. 4). Interestingly, treatment of tachyzoites with the FASII inhibitor triclosan or inactivating the FASII component acyl carrier protein was shown to lead to severe problems in cytokinesis completion, with tethered daughter cells resembling the phenotype we have described here (49). A similar phenotype was also observed in the mutant for TgATS2, an apicoplast-located acyltransferase responsible for phosphatidic acid synthesis (46). This points to a central role for the apicoplast to provide specific precursors for membrane biogenesis during cytokinesis and to a SUF-dependent FASII function is important for the homeostasis of the parasite plasma membrane. It should however be noted that some isoprenoid-dependent cellular mediators may also contribute to plasma membrane synthesis during cell division. For instance, disruption of Rab-controlled vesicular trafficking leads to very similar phenotypes of incomplete cytokinesis, with tachyzoites still fused along their lateral surface (74, 75). Glycosylated IMC proteins associated with gliding motility are also important for IMC formation and the cell division process (77). It is also possible that yet unidentified GPI-anchored *T. gondii* proteins may be involved in plasma membrane formation or recycling: GPI synthesis is essential for *T. gondii* survival (78), but the function of individual GPI-anchored proteins remains largely overlooked. The detrimental effects of SUF depletion on plasma membrane homeostasis may thus manifest through both FASII and isoprenoid perturbation. Moreover, as some isoprenoid-dependent modifications are also linked to FA acid synthesis, like GPI anchors of *T. gondii* surface proteins that also

necessitate phospholipid moieties (79), a simultaneous impact on the two pathways may enhance the phenotypic output.

One key apicoplast-located Fe-S protein is Fd, which has a central role in the function of Fe-S–dependent apicoplast enzymes: it is potentially providing electrons to other apicoplast Fe-S enzymes like MiaB, IspG, IspH, and LipA. The role of Fd has recently been investigated in Apicomplexa. In *Plasmodium* blood stages, the loss of parasite viability upon Fd depletion was likely mostly due to the importance of Fd for the isoprenoid synthesis pathway (40), which is the only essential apicoplast-located pathway in this developmental stage. Fd is equally essential for *T. gondii*, tachyzoite survival, where it was shown to impact both FASII and isoprenoid synthesis (38), in a similar fashion to the SUF mutants we describe here. Whether the vital importance of Fe-S cluster synthesis and associated apicoplast redox metabolism is solely through its key role in isoprenoid synthesis is thus less clear in *T. gondii* than in *Plasmodium*. As *T. gondii* tachyzoites grow in host cell types that can potentially provide them with more resources, the ability to scavenge exogenous metabolites creates a complex situation whereby metabolic pathways like FASII may be only essential in certain particular conditions. The nutrient-rich *in vitro* culture systems may also mask some important contributions. In any case, because of their upstream role in cellular functions important for parasite fitness, Fd and SUF mutants clearly have pleiotropic defects. More importantly, we have confirmed here that disrupting the SUF machinery leads to an irreversible death of the tachyzoites, which is not the case, for example, when the mitochondrial Fe-S cluster machinery is inactivated (14). For all these reasons, and also because of its absence from mammalian hosts of the parasite, the SUF pathway has a strong potential for identifying novel drug targets.

Experimental procedures

Parasites and cells culture

Tachyzoites of the TATi ΔKu80 *T. gondii* strain (28), as well as derived transgenic parasites generated in this study, were maintained by serial passage in monolayers of human foreskin fibroblast (HFF, American Type Culture Collection, CRL 1634) grown in Dulbecco's modified Eagle medium (DMEM, Gibco), supplemented with 5% decomplemented fetal bovine serum, 2-mM L-glutamine, and a cocktail of penicillin-streptomycin at 100 μg/ml.

Bioinformatic analyses

Sequence alignment was performed using the MUltiple Sequence Comparison by Log-Expectation algorithm of the Geneious 6.1.8 software suite (http://www.geneious.com/). Transit peptide and localization prediction was done with the Deeploc 1.0 (https://services.healthtech.dtu.dk/service.php?DeepLoc-1.0) algorithm.

Heterologous expression *in* E. coli

Construct for designing the recombinant protein used for *E. coli* complementation was defined by aligning the amino acid sequences of TgSUFC with its *E. coli* counterparts. An 894 bp fragment corresponding to amino acids 220 to 518 was amplified by PCR from *T. gondii* cDNA using primers ML4200/ML4010 (sequences of the primers used in this study are found in Table S1). The fragment was cloned into the pUC19 plasmid (Thermo Fisher Scientific) using the HindIII/BamHI restriction sites. The SufC *E. coli* mutant from the Keio collection (obtained from 'The *Coli* Genetic Stock Center at the University of Yale': strain number JW1672-1) was transformed with the plasmid expressing the TgSUFC recombinant protein and selected with ampicillin. For growth assays (25), overnight stationary phase cultures were adjusted to the same density starting with an A_{600} of 0.6 in salt-supplemented M9 minimal media containing 0.4% glucose and varying amounts of the 2,2′-Bipyridyl iron chelator (Sigma-Aldrich). Growth was monitored through A_{600} measurement after 7, 14, and 24 h at 37 °C in a shaking incubator.

Generation of the HA-tagged TgSUFC cell line

A CRISPR-based strategy was used. Using the pLIC-HA_3-CAT plasmid as a template, a PCR was performed with the KOD DNA polymerase (Novagen) to amplify the tag and the resistance gene expression cassette with primers ML3980/ML3981 that also carry 30 bp homology with the 3′ end of the corresponding genes. A specific single-guide RNA was generated to introduce a double-stranded break at the 3′ of the *TgSUFC* gene, using primers ML3952/ML3953, and the protospacer sequences were introduced in the Cas9-expressing pU6-Universal plasmid (Addgene, ref #52694) (41). The TATi ΔKu80 cell line was transfected and transgenic parasites were selected with 20 μM chloramphenicol (Sigma-Aldrich) and cloned by serial limiting dilution.

Generation of TgSUFC conditional knockdown and complemented cell lines

The conditional knockdown cell line for *TgSUFC* was generated based on the Tet-Off system using the DHFR-TetO7Sag4 plasmid (80) using a CRISPR-based strategy. Using the DHFR-TetO7Sag4 plasmid as a template, a PCR was performed with the KOD DNA polymerase (Novagen) to amplify the promoter and the resistance gene expression cassette with primers ML4107/ML4108 that also carry 30 bp homology with the 5′ end of the *TgSUFC* gene. A specific single-guide RNA was generated to introduce a double-stranded break at the 5′ of the *TgSUFC* locus. Primers used to generate the guide were ML4109/ML4110, and the protospacer sequences were introduced in the pU6-Universal plasmid (Addgene ref #52694) (41). The TgSUFC-HA cell line was transfected with the donor sequence, and the Cas9/guide RNA-expressing pU6-Universal plasmid, and transgenic parasites were selected with 1 μM pyrimethamine (Sigma-Aldrich) and cloned by serial limiting dilution.

The cKD TgSUFC-HA cell line was complemented by the addition of an extra copy of the *TgSUFC* gene put under the dependence of a tubulin promoter at the *UPRT* locus. The whole *TgSUFC* cDNA sequence (1557 bp) was amplified by RT-PCR with primers ML4815/ML4816. It was then cloned

downstream of the *tubulin* promoter sequence of the pUPRT-TUB-Ty vector (28) to yield the pUPRT-TgSUFC plasmid. This plasmid was then linearized prior to transfection of the mutant cell line. The recombination efficiency was increased by cotransfecting with the Cas9-expressing pU6-UPRT plasmids generated by integrating *UPRT*-specific protospacer sequences (with primers ML2087/ML2088 for the 3′ and primers ML3445/ML3446 for the 5′), which were designed to allow a double-strand break at the *UPRT* locus. Transgenic parasites were selected using 5 μM 5-fluorodeoxyuridine (Sigma-Aldrich) and cloned by serial limiting dilution to yield the cKD TgSUFC-HA comp cell line.

Anti–TgPDH-E2 antibody production

A polyclonal antibody was raised in rabbit against a peptide (ISLIQAKGLSLISASSSPA) specific of TgPDH-E2 by the Proteogenix company. The peptide was conjugated to Keyhole limpet hemocyanin carrier protein prior to immunization, and the whole serum was affinity-purified against the peptide for increased specificity. The specificity of the antibody was verified by immunoblot and IFA (Fig. S5).

Immunoblot analysis

Protein extracts from 10^7 freshly egressed tachyzoites were prepared in Laemmli sample buffer, separated by SDS-PAGE on a 10% acrylamide gel and transferred onto nitrocellulose membrane using the BioRad Mini-Transblot system according to the manufacturer's instructions. Membranes were blocked in tris-buffered saline with 0.1% v/v Tween-20 and 5% w/v nonfat dry milk and were subsequently incubated with antibodies in the same solution. Rat monoclonal antibody (clone 3F10, Roche) was used at 1/500 to detect HA-tagged proteins. Other primary antibodies used were mouse monoclonal anti-TY tag (30) (hybridoma supernatant used at 1/20), rabbit anti-lipoic acid antibody (ab58724, Abcam) used at 1/300, mouse anti-SAG1 (81) used at 1/1000, mouse anti-actin (82) (hybridoma supernatant used at 1/25), rabbit anti-PDH E2 (this study, used at 1/500), and rabbit anti-farnesyl polyclonal antibody (PA1-12554, Life Technologies) used at 1/300.

Immunofluorescence microscopy

For IFAs, intracellular tachyzoites grown on coverslips containing HFF monolayers were either fixed for 20 min with 4% (w/v) paraformaldehyde (PFA) in PBS and permeabilized for 10 min with 0.3% Triton X-100 in PBS, or fixed for 5 min in cold methanol (for SAG labeling). Slides/coverslips were subsequently blocked with 1% (w/v) bovine serum albumin in PBS. Primary antibodies used (at 1/1,000, unless specified) were rat anti-HA tag (clone 3F10, Roche), mouse anti-TY tag (30) (hybridoma supernatant used at 1/20), rabbit anti-CPN60 (83), rabbit anti-IMC3 (84), mouse anti-SAG1 (81), and mouse anti-SAG3 (85). Staining of DNA was performed on fixed cells by incubating them for 5 min in a 1 μg/ml 4,6-diamidino-2-phenylindole solution. All images were acquired at the Montpellier RIO imaging facility from a Zeiss AXIO Imager Z2 epifluorescence microscope driven by the ZEN software v2.3 (Zeiss). Z-stack acquisition and maximal intensity projection was performed to quantify apicoplast loss. Adjustments for brightness and contrast were applied uniformly on the entire image.

Electron microscopy

Parasites were pretreated for 3 days with ATc (Sigma-Aldrich) at 1 μg/ml (the concentration used throughout this study, unless specified) and then used to infect HFF monolayers and grown for an extra 24 h in ATc. Untreated parasites were used as a control for normal morphology. They were fixed with 2.5% glutaraldehyde in cacodylate buffer 0.1 M pH7.4. Coverslips were then processed using a Pelco Biowave pro+ (Ted Pella). Briefly, samples were postfixed in 1% OsO_4 and 2% uranyl acetate, dehydrated in acetonitrile series, and embedded in Epon 118 using the following parameters: glutaraldehyde (150 W ON/OFF/ON 1-min cycles); two buffer washes (40 s 150 W); OsO_4 (150 W ON/OFF/ON/OFF/ON 1-min cycles); two water washes (40 s 150 W); uranyl acetate (100 W ON/OFF/ON 1-min cycles); dehydration (40 s 150 W); resin infiltration (350 W 3-min cycles). Fixation and infiltration steps were performed under vacuum. Polymerization was performed at 60 °C for 48 h. Ultrathin sections at 70 nM were cut with a Leica UC7 ultramicrotome, counterstained with uranyl acetate and lead citrate, and observed in a Jeol 1400+ transmission electron microscope from the MEA Montpellier Electron Microscopy Platform. All chemicals were from Electron Microscopy Sciences, and solvents were from Sigma-Aldrich.

Plaque assay

Confluent monolayers of HFFs were infected with freshly egressed parasites, which were left to grow for 7 days in the absence or presence of ATc (unless stated). For some experiments, the medium was supplemented with 50 μM palmitic acid (P0500, Sigma-Aldrich), 50 μM myristic acid (70,082, Sigma-Aldrich), or 20 μM geranylgeraniol (G3278, Sigma-Aldrich). They were then fixed with 4% v/v PFA, and plaques were revealed by staining with a 0.1% crystal violet solution (V5265, Sigma-Aldrich). Images of the plaques were acquired with an Olympus MVX10 stereomicroscope, and plaque area was measured using the Zen 2.3 software (Zeiss) with the "contour" tool.

Gliding assay

10^7 freshly egressed parasites were resuspended in 300 μl of motility buffer (Ringer's solution: 155 mM NaCl, 3 mM KCl, 2 mM $CaCl_2$, 1 mM $MgCl_2$, 3 mM NaH_2PO_4, 10 mM Hepes, 10 mM glucose). Hundred microliters were deposited on poly-L-lysine coated microscope slides (J2800AMNZ, Thermo Scientific), in a well delineated with a hydrophobic pen (PAP Pen, Kisker Biotech). Parasites were left to glide for 15 min in an incubator at 37 °C, then the suspension was carefully removed and parasites were fixed with 4% (w/v) PFA in PBS.

Immunostaining was performed with an anti-SAG1 antibody (81) as described above, but without permeabilization. Alternatively, trails were stained with the DiI perchlorate lipophilic membrane stain (D282, Invitrogen). The gliding assay was performed as described above, with the modification that DiI was added at a final concentration of 10 μM directly in the Ringer's solution for the duration of the gliding assay (15 min), prior to fixation with 4% (w/v) PFA in PBS and further processing for microscopic imaging.

Trail deposition images were acquired with a 63× objective on a Zeiss AXIO Imager Z2 epifluorescence microscope and processed with ImageJ v. 1.53f51, using the NeuronJ plugin as described previously (38).

Analysis of FA content

Parasite GC-MS analyses were conducted as previously described (46, 47). Briefly, the parasites were grown for 72 h in ± ATc conditions within a confluent monolayer of HFF in flasks (175 cm^2). At each time point, parasites were harvested as intracellular tachyzoites (1×10^7 cell equivalents per replicate) after syringe filtration with 3-μm pore size membrane. These parasites were metabolically quenched by rapid chilling in a dry ice-ethanol slurry bath and then centrifuged down at 4 °C. The parasite pellet was washed with ice-cold PBS thrice. Then, total lipids were extracted in chloroform/methanol/water (1:3:1, v/v/v) containing PC (C13:0/C13:0), 10 nmol, and C21:0 (10 nmol) as internal standards for extraction. Polar and apolar metabolites were separated by phase partitioning by adding chloroform and water to give the ratio of chloroform/methanol/water as 2:1:0.8 (v/v/v). For lipid analysis, the organic phase was dried under N_2 gas and dissolved in 1-butanol to obtain 1 μl butanol/10^7 parasites.

Total FA content analysis

The extracted total lipid sample was then added with 1 nmol pentadecanoic acid (C15:0) as internal standard as stated before using trimethylsulfonium hydroxide for total FA content. Resultant FA methyl esters (FAMEs) were analyzed by GC-MS as previously described (45). All FAMEs were identified by comparison of retention time and mass spectra from GC-MS with authentic chemical standards. The concentration of FAMEs was quantified after initial normalization to different internal standards and finally to parasite number.

Tracking host-derived FAs—(monitoring parasite scavenging capacities)

Stable isotope metabolic labeling combined to GC-MS analyses have been conducted as previously established and described (47). Briefly, the HFF cells were grown (1×10^8 cell equivalents per replicate) to confluency in the presence of stable U-^{13}C-glucose isotope at a final concentration of 800 μM added to a glucose-free DMEM. These ^{13}C-prelabeled HFF were then infected with TgNFS2/TgSUFC cKD parasites in the presence of normal-glucose–containing DMEM under ± ATc (0.5 μg/ml). The host HFF and parasites were metabolically quenched separately, and their FA content was quantified by GC-MS as described above. As described previously, the degree of the incorporation of ^{13}C into FAs (%carbon incorporation) is determined by the mass isotopomer distribution of each FAMEs. The total abundance of ^{13}C-labeled FAs was analyzed initially for HFF to check labeling of the metabolites (described previously). Later, the same was calculated for parasites to confirm direct uptake of ^{13}C-labeled FAs from the host.

Statistical analyses

All statistical analyses were performed with the Prism 8 software (Graphpad) using two-tailed Student's *t* test comparisons.

Data availability

All data are contained within the article. Material described is available upon request from the corresponding author.

Supporting information—This article contains supporting information.

Acknowledgments—We are grateful to B. Striepen, L. Sheiner, S. Lourido, D. Soldati-Favre, M.J. Gubbels, V. Carruthers, and J.F. Dubremetz for sharing antibodies, strains, and plasmids. We wish to thank K. Semenovskaya for technical help with some constructs. We also thank the Montpellier Rio Imaging facility for providing access to their microscopes, as well as the electron microscopy imaging facility of the University of Montpellier.

Author contributions—E. A. R., S. P., A. C., L. B., C. L.-V., Y. Y.-B., and S. B. investigation; E. A. R. validation; C. L.-V., Y. Y.-B., and S. B. formal analysis; C. L.-V. and S. B. visualization; C. Y. B. and S. B. resources; C. Y. B. and S. B. supervision; C. Y. B. writing–review and editing; C. Y. B. and S. B. funding acquisition; S. B. conceptualization; S. B. writing–original draft.

Funding and additional information—A. C. was supported by a fellowship from the Fondation pour la Recherche Médicale (Equipe FRM EQ20170336725), as well as C. L.-V., C. Y. B., and Y. Y.-B. (Equipe FRM EQU202103012700). C. Y. B. and S. B. acknowledge support from the Labex Parafrap (ANR-11-LABX-0024), the Agence Nationale de la Recherche (ANR-21-CE44-0010 to C. Y. B. and S. B. and ANR-19-CE15–0023 to S. B.). Funding from the Région Auvergne Rhône-Alpes for the lipidomics analyses platform is also acknowledged (Grant IRICE Project GEMELI). The funders had no role in study design, data collection and analysis, decision to publish, or preparation of the article.

Conflict of interest—The authors declare that they have no conflicts of interest with the contents of this article.

Abbreviations—The abbreviations used are: ATc, anhydrotetracycline; cKD, conditional knockdown; DiI, 1,1′-dioctadecyl-3,3,3′,3′-tetramethylindocarbocyanine; ETC, electron transport chain; FA, fatty acid; FAME, FA methyl ester; FASII, type II fatty acid synthase; Fd, ferredoxin; Fe-S, iron-sulfur; GGOH, geranylgeraniol; GPI, glycosylphosphatidylinositol; HA, hemagglutinin; HFF, human foreskin fibroblast; IFA, immunofluorescence assay; IMC, inner membrane complex; IPP, isopentenyl pyrophosphate; ISC, iron-sulfur cluster; LipA, lipoyl synthase; PDH, pyruvate dehydrogenase; SAG, surface antigen; SUF, sulfur utilization factor;

TATi, tetracycline-inducible transactivator; UPRT, uracil phosphoribosyltransferase.

References

1. White, N. J., Pukrittayakamee, S., Hien, T. T., Faiz, M. A., Mokuolu, O. A., and Dondorp, A. M. (2014) Malaria. *Lancet* **383**, 723–735
2. Sanchez, S. G., and Besteiro, S. (2021) The pathogenicity and virulence of Toxoplasma gondii. *Virulence* **12**, 3095–3114
3. Janouskovec, J., Horak, A., Obornik, M., Lukes, J., and Keeling, P. J. (2010) A common red algal origin of the apicomplexan, dinoflagellate, and heterokont plastids. *Proc. Natl. Acad. Sci. U. S. A.* **107**, 10949–10954
4. van Dooren, G. G., and Striepen, B. (2013) The algal past and parasite present of the apicoplast. *Annu. Rev. Microbiol.* **67**, 271–289
5. van Dooren, G. G., and Hapuarachchi, S. V. (2017) The dark side of the chloroplast: biogenesis, metabolism and membrane biology of the apicoplast. *Adv. Bot. Res.* **84**, 145–185
6. Seeber, F., and Soldati-Favre, D. (2010) Metabolic pathways in the apicoplast of apicomplexa. *Int. Rev. Cell Mol. Biol.* **281**, 161–228
7. Biddau, M., and Sheiner, L. (2019) Targeting the apicoplast in malaria. *Biochem. Soc. Trans.* **47**, 973–983
8. Kennedy, K., Crisafulli, E. M., and Ralph, S. A. (2019) Delayed death by plastid inhibition in apicomplexan parasites. *Trends Parasitol.* **35**, 747–759
9. Uddin, T., McFadden, G. I., and Goodman, C. D. (2018) Validation of putative apicoplast-targeting drugs using a chemical supplementation assay in cultured human malaria parasites. *Antimicrob. Agents Chemother.* **62**, e01161-17
10. Imlay, J. A. (2006) Iron-sulphur clusters and the problem with oxygen. *Mol. Microbiol.* **59**, 1073–1082
11. Lill, R. (2009) Function and biogenesis of iron–sulphur proteins. *Nature* **460**, 831–838
12. Braymer, J. J., Freibert, S. A., Rakwalska-Bange, M., and Lill, R. (2021) Mechanistic concepts of iron-sulfur protein biogenesis in Biology. *Biochim. Biophys. Acta (Bba) - Mol. Cell Res.* **1868**, 118863
13. Aw, Y. T. V., Seidi, A., Hayward, J. A., Lee, J., Victor Makota, F., Rug, M., *et al.* (2020) A key cytosolic iron-sulfur cluster synthesis protein localises to the mitochondrion of Toxoplasma gondii. *Mol. Microbiol.* **115**, 968–985
14. Pamukcu, S., Cerutti, A., Bordat, Y., Hem, S., Rofidal, V., and Besteiro, S. (2021) Differential contribution of two organelles of endosymbiotic origin to iron-sulfur cluster synthesis and overall fitness in Toxoplasma. *PLoS Pathog.* **17**, e1010096
15. Gisselberg, J. E., Dellibovi-Ragheb, T. A., Matthews, K. A., Bosch, G., and Prigge, S. T. (2013) The Suf iron-sulfur cluster synthesis pathway is required for apicoplast maintenance in malaria parasites. *PLoS Pathog.* **9**, e1003655
16. Haussig, J. M., Matuschewski, K., and Kooij, T. W. A. (2014) Identification of vital and dispensable sulfur utilization factors in the Plasmodium apicoplast. *PLoS One* **9**, e89718
17. Kumar, B., Chaubey, S., Shah, P., Tanveer, A., Charan, M., Siddiqi, M. I., *et al.* (2011) Interaction between sulphur mobilisation proteins SufB and SufC: evidence for an iron–sulphur cluster biogenesis pathway in the apicoplast of Plasmodium falciparum. *Int. J. Parasitol.* **41**, 991–999
18. Charan, M., Singh, N., Kumar, B., Srivastava, K., Siddiqi, M. I., and Habib, S. (2014) Sulfur mobilization for Fe-S cluster assembly by the essential SUF pathway in the Plasmodium falciparum apicoplast and its inhibition. *Antimicrob. Agents Chemother.* **58**, 3389–3398
19. Charan, M., Choudhary, H. H., Singh, N., Sadik, M., Siddiqi, M. I., Mishra, S., *et al.* (2017) [Fe-S] cluster assembly in the apicoplast and its indispensability in mosquito stages of the malaria parasite. *FEBS J.* **284**, 2629–2648
20. Takahashi, Y., and Tokumoto, U. (2002) A third bacterial system for the assembly of iron-sulfur clusters with homologs in archaea and plastids. *J. Biol. Chem.* **277**, 28380–28383
21. Hirabayashi, K., Yuda, E., Tanaka, N., Katayama, S., Iwasaki, K., Matsumoto, T., *et al.* (2015) Functional dynamics revealed by the structure of the SufBCD complex, a novel ATP-binding cassette (ABC) protein that serves as a scaffold for Iron-Sulfur cluster biogenesis. *J. Biol. Chem.* **290**, 29717–29731
22. Harb, O. S., and Roos, D. S. (2020) ToxoDB: functional genomics resource for Toxoplasma and related organisms. *Met. Mol. Biol.* **2071**, 27–47
23. Almagro Armenteros, J. J., Sønderby, C. K., Sønderby, S. K., Nielsen, H., and Winther, O. (2017) DeepLoc: prediction of protein subcellular localization using deep learning. *Bioinformatics* **33**, 3387–3395
24. Barylyuk, K., Koreny, L., Ke, H., Butterworth, S., Crook, O. M., Lassadi, I., *et al.* (2020) A comprehensive subcellular atlas of the Toxoplasma proteome *via* hyperLOPIT provides spatial context for protein functions. *Cell Host & Microbe* **28**, 752–766.e9. https://doi.org/10.1016/j.chom.2020.09.011
25. Outten, F. W., Djaman, O., and Storz, G. (2004) A suf operon requirement for Fe-S cluster assembly during iron starvation in Escherichia coli: suf operon role during iron starvation. *Mol. Microbiol.* **52**, 861–872
26. Fox, B. A., Ristuccia, J. G., Gigley, J. P., and Bzik, D. J. (2009) Efficient gene replacements in Toxoplasma gondii strains deficient for nonhomologous end joining. *Eukaryot. Cell* **8**, 520–529
27. Huynh, M.-H., and Carruthers, V. B. (2009) Tagging of endogenous genes in a Toxoplasma gondii strain lacking Ku80. *Eukaryot. Cell* **8**, 530–539
28. Sheiner, L., Demerly, J. L., Poulsen, N., Beatty, W. L., Lucas, O., Behnke, M. S., *et al.* (2011) A systematic screen to discover and analyze apicoplast proteins identifies a conserved and essential protein import factor. *PLoS Pathog.* **7**, e1002392
29. Meissner, M., Brecht, S., Bujard, H., and Soldati, D. (2001) Modulation of myosin A expression by a newly established tetracycline repressor-based inducible system in Toxoplasma gondii. *Nucl. Acids Res.* **29**, E115
30. Bastin, P., Bagherzadeh, A., Matthews, K. R., and Gull, K. (1996) A novel epitope tag system to study protein targeting and organelle biogenesis in Trypanosoma brucei. *Mol. Biochem. Parasitol.* **77**, 235–239
31. Francia, M. E., and Striepen, B. (2014) Cell division in apicomplexan parasites. *Nat. Rev. Microbiol.* **12**, 125–136
32. Harding, C. R., and Meissner, M. (2014) The inner membrane complex through development of Toxoplasma gondii and Plasmodium. *Cell Microbiol.* **16**, 632–641
33. Ouologuem, D. T., and Roos, D. S. (2014) Dynamics of the Toxoplasma gondii inner membrane complex. *J. Cell Sci.* **127**, 3320–3330
34. Gubbels, M.-J., Wieffer, M., and Striepen, B. (2004) Fluorescent protein tagging in Toxoplasma gondii: identification of a novel inner membrane complex component conserved among apicomplexa. *Mol. Biochem. Parasitol.* **137**, 99–110
35. Imlay, L., and Odom, A. R. (2014) Isoprenoid metabolism in apicomplexan parasites. *Curr. Clin. Microbiol. Rep.* **1**, 37–50
36. Thomsen-Zieger, N., Schachtner, J., and Seeber, F. (2003) Apicomplexan parasites contain a single lipoic acid synthase located in the plastid. *FEBS Lett.* **547**, 80–86
37. Pierrel, F., Douki, T., Fontecave, M., and Atta, M. (2004) MiaB protein is a bifunctional radical-S-adenosylmethionine enzyme involved in thiolation and methylation of tRNA. *J. Biol. Chem.* **279**, 47555–47563
38. Henkel, S., Frohnecke, N., Maus, D., McConville, M. J., Laue, M., Blume, M., *et al.* (2022) Toxoplasma gondii apicoplast-resident ferredoxin is an essential electron transfer protein for the MEP isoprenoid-biosynthetic pathway. *J. Biol. Chem.* **298**, 101468
39. Frohnecke, N., Klein, S., and Seeber, F. (2015) Protein–protein interaction studies provide evidence for electron transfer from ferredoxin to lipoic acid synthase in *Toxoplasma gondii*. *FEBS Lett.* **589**, 31–36
40. Swift, R. P., Rajaram, K., Elahi, R., Liu, H. B., and Prigge, S. T. (2022) Roles of ferredoxin-dependent proteins in the apicoplast of Plasmodium falciparum parasites. *mBio* **13**, e0302321
41. Sidik, S. M., Huet, D., Ganesan, S. M., Huynh, M.-H., Wang, T., Nasamu, A. S., *et al.* (2016) A genome-wide CRISPR screen in Toxoplasma identifies essential apicomplexan genes. *Cell* **166**, 1423–1435.e12
42. Jelenska, J., Crawford, M. J., Harb, O. S., Zuther, E., Haselkorn, R., Roos, D. S., *et al.* (2001) Subcellular localization of acetyl-CoA carboxylase in the apicomplexan parasite Toxoplasma gondii. *Proc. Natl. Acad. Sci. U. S. A.* **98**, 2723–2728

43. Mazumdar, J., H Wilson, E., Masek, K., A Hunter, C., and Striepen, B. (2006) Apicoplast fatty acid synthesis is essential for organelle biogenesis and parasite survival in Toxoplasma gondii. *Proc. Natl. Acad. Sci. U. S. A.* **103**, 13192–13197
44. Ramakrishnan, S., Docampo, M. D., Macrae, J. I., Pujol, F. M., Brooks, C. F., van Dooren, G. G., *et al.* (2012) Apicoplast and endoplasmic reticulum cooperate in fatty acid biosynthesis in apicomplexan parasite Toxoplasma gondii. *J. Biol. Chem.* **287**, 4957–4971
45. Dubois, D., Fernandes, S., Amiar, S., Dass, S., Katris, N. J., Botté, C. Y., *et al.* (2018) Toxoplasma gondii acetyl-CoA synthetase is involved in fatty acid elongation (of long fatty acid chains) during tachyzoite life stages. *J. Lipid Res.* **59**, 994–1004
46. Amiar, S., Katris, N. J., Berry, L., Dass, S., Duley, S., Arnold, C.-S., *et al.* (2020) Division and adaptation to host environment of apicomplexan parasites depend on apicoplast lipid metabolic plasticity and host organelle remodeling. *Cell Rep.* **30**, 3778–3792.e9
47. Dass, S., Shunmugam, S., Berry, L., Arnold, C.-S., Katris, N. J., Duley, S., *et al.* (2021) Toxoplasma LIPIN is essential in channeling host lipid fluxes through membrane biogenesis and lipid storage. *Nat. Commun.* **12**, 2813
48. Liang, X., Cui, J., Yang, X., Xia, N., Li, Y., Zhao, J., *et al.* (2020) Acquisition of exogenous fatty acids renders apicoplast-based biosynthesis dispensable in tachyzoites of Toxoplasma. *J. Biol. Chem.* **295**, 7743–7752
49. Martins-Duarte, É. S., Carias, M., Vommaro, R., Surolia, N., and de Souza, W. (2016) Apicoplast fatty acid synthesis is essential for pellicle formation at the end of cytokinesis in Toxoplasma gondii. *J. Cell Sci.* **129**, 3320–3331
50. Yeh, E., and DeRisi, J. L. (2011) Chemical rescue of malaria parasites lacking an apicoplast defines organelle function in blood-stage Plasmodium falciparum. *PLoS Biol.* **9**, e1001138
51. Nair, S. C., Brooks, C. F., Goodman, C. D., Sturm, A., Strurm, A., McFadden, G. I., *et al.* (2011) Apicoplast isoprenoid precursor synthesis and the molecular basis of fosmidomycin resistance in Toxoplasma gondii. *J. Exp. Med.* **208**, 1547–1559
52. Li, Z.-H., Ramakrishnan, S., Striepen, B., and Moreno, S. N. J. (2013) Toxoplasma gondii relies on both host and parasite isoprenoids and can be rendered sensitive to Atorvastatin. *PLoS Pathog.* **9**, e1003665
53. Kennedy, K., Cobbold, S. A., Hanssen, E., Birnbaum, J., Spillman, N. J., McHugh, E., *et al.* (2019) Delayed death in the malaria parasite Plasmodium falciparum is caused by disruption of prenylation-dependent intracellular trafficking. *PLoS Biol.* **17**, e3000376
54. Li, Z.-H., King, T. P., Ayong, L., Asady, B., Cai, X., Rahman, T., *et al.* (2021) A plastid two-pore channel essential for inter-organelle communication and growth of Toxoplasma gondii. *Nat. Commun.* **12**, 5802
55. Suazo, K. F., Schaber, C., Palsuledesai, C. C., Odom John, A. R., and Distefano, M. D. (2016) Global proteomic analysis of prenylated proteins in Plasmodium falciparum using an alkyne-modified isoprenoid analogue. *Sci. Rep.* **6**, 38615
56. Gisselberg, J. E., Zhang, L., Elias, J. E., and Yeh, E. (2017) The prenylated proteome of Plasmodium falciparum reveals pathogen-specific prenylation activity and drug mechanism-of-action. *Mol. Cell Proteomics* **16**, S54–S64
57. Jung, C., Lee, C. Y.-F., and Grigg, M. E. (2004) The SRS superfamily of Toxoplasma surface proteins. *Int. J. Parasitol.* **34**, 285–296
58. Striepen, B., Yingxin He, C., Matrajt, M., Soldati, D., and Roos, D. S. (1998) Expression, selection, and organellar targeting of the green fluorescent protein in Toxoplasma gondii. *Mol. Biochem. Parasitol.* **92**, 325–338
59. Fauquenoy, S., Morelle, W., Hovasse, A., Bednarczyk, A., Slomianny, C., Schaeffer, C., *et al.* (2008) Proteomics and glycomics analyses of N-glycosylated structures involved in Toxoplasma gondii-host cell interactions. *Mol. Cell Proteomics* **7**, 891–910
60. Luk, F. C. Y., Johnson, T. M., and Beckers, C. J. (2008) N-linked glycosylation of proteins in the protozoan parasite Toxoplasma gondii. *Mol. Biochem. Parasitol.* **157**, 169–178
61. Albuquerque-Wendt, A., Jacot, D., Dos Santos Pacheco, N., Seegers, C., Zarnovican, P., Buettner, F. F. R., *et al.* (2020) C-Mannosylation of Toxoplasma gondii proteins promotes attachment to host cells and parasite virulence. *J. Biol. Chem.* **295**, 1066–1076
62. Håkansson, S., Morisaki, H., Heuser, J., and Sibley, L. D. (1999) Time-lapse video microscopy of gliding motility in Toxoplasma gondii reveals a novel, biphasic mechanism of cell locomotion. *Mol. Biol. Cell* **10**, 3539–3547
63. Vaughan, A. M., O'Neill, M. T., Tarun, A. S., Camargo, N., Phuong, T. M., Aly, A. S. I., *et al.* (2009) Type II fatty acid synthesis is essential only for malaria parasite late liver stage development. *Cell Microbiol.* **11**, 506–520
64. Primo, V. A., Rezvani, Y., Farrell, A., Murphy, C. Q., Lou, J., Vajdi, A., *et al.* (2021) The extracellular milieu of Toxoplasma's lytic cycle drives lab adaptation, primarily by transcriptional reprogramming. *mSystems* **6**, e0119621
65. Xu, X.-P., Elsheikha, H. M., Liu, W.-G., Zhang, Z.-W., Sun, L.-X., Liang, Q.-L., *et al.* (2021) The role of type II fatty acid synthesis enzymes FabZ, ODSCI, and ODSCII in the pathogenesis of Toxoplasma gondii infection. *Front. Microbiol.* **12**, 703059
66. Shunmugam, S., Arnold, C.-S., Dass, S., Katris, N. J., and Botté, C. Y. (2022) The flexibility of Apicomplexa parasites in lipid metabolism. *PLoS Pathog.* **18**, e1010313
67. Krishnan, A., Kloehn, J., Lunghi, M., Chiappino-Pepe, A., Waldman, B. S., Nicolas, D., *et al.* (2020) Functional and computational genomics reveal unprecedented flexibility in stage-specific Toxoplasma metabolism. *Cell Host & Microbe* **27**, 290–306.e11
68. Amberg-Johnson, K., and Yeh, E. (2019) Host cell metabolism contributes to delayed-death kinetics of apicoplast inhibitors in Toxoplasma gondii. *Antimicrob. Agents Chemother.* **63**, e01646-18
69. Baggish, A. L., and Hill, D. R. (2002) Antiparasitic agent atovaquone. *Antimicrob. Agents Chemother.* **46**, 1163–1173
70. Huet, D., Rajendran, E., van Dooren, G. G., and Lourido, S. (2018) Identification of cryptic subunits from an apicomplexan ATP synthase. *eLife* **7**, e38097
71. Seidi, A., Muellner-Wong, L. S., Rajendran, E., Tjhin, E. T., Dagley, L. F., Aw, V. Y., *et al.* (2018) Elucidating the mitochondrial proteome of Toxoplasma gondii reveals the presence of a divergent cytochrome c oxidase. *Elife* **7**, e38131
72. Hayward, J. A., Rajendran, E., Zwahlen, S. M., Faou, P., and van Dooren, G. G. (2021) Divergent features of the coenzyme Q:cytochrome c oxidoreductase complex in Toxoplasma gondii parasites. *PLoS Pathog.* **17**, e1009211
73. Maclean, A. E., Bridges, H. R., Silva, M. F., Ding, S., Ovciarikova, J., Hirst, J., *et al.* (2021) Complexome profile of Toxoplasma gondii mitochondria identifies divergent subunits of respiratory chain complexes including new subunits of cytochrome bc1 complex. *PLoS Pathog.* **17**, e1009301
74. Agop-Nersesian, C., Naissant, B., Ben Rached, F., Rauch, M., Kretzschmar, A., Thiberge, S., *et al.* (2009) Rab11A-controlled assembly of the inner membrane complex is required for completion of apicomplexan cytokinesis. *PLoS Pathog.* **5**, e1000270
75. Venugopal, K., Chehade, S., Werkmeister, E., Barois, N., Periz, J., Lafont, F., *et al.* (2020) Rab11A regulates dense granule transport and secretion during Toxoplasma gondii invasion of host cells and parasite replication. *PLoS Pathog.* **16**, e1008106
76. Okada, M., Rajaram, K., Swift, R. P., Mixon, A., Maschek, J. A., Prigge, S. T., *et al.* (2021) Critical role for isoprenoids in apicoplast biogenesis by malaria parasites. *Microbiology* **11**, e73208
77. Harding, C. R., Egarter, S., Gow, M., Jiménez-Ruiz, E., Ferguson, D. J. P., and Meissner, M. (2016) Gliding associated proteins play essential roles during the formation of the inner membrane complex of Toxoplasma gondii. *PLoS Pathog.* **12**, e1005403
78. Wichroski, M. J., and Ward, G. E. (2003) Biosynthesis of glycosylphosphatidylinositol Is essential to the survival of the protozoan parasite Toxoplasma gondii. *Eukaryot. Cell* **2**, 1132–1136
79. Tomavo, S., Schwarz, R. T., and Dubremetz, J. F. (1989) Evidence for glycosyl-phosphatidylinositol anchoring of Toxoplasma gondii major surface antigens. *Mol. Cell. Biol.* **9**, 4576–4580
80. Morlon-Guyot, J., Berry, L., Chen, C.-T., Gubbels, M.-J., Lebrun, M., and Daher, W. (2014) The Toxoplasma gondii calcium-dependent protein kinase 7 is involved in early steps of parasite division and is crucial for parasite survival. *Cell. Microbiol.* **16**, 95–114

81. Couvreur, G., Sadak, A., Fortier, B., and Dubremetz, J. F. (1988) Surface antigens of Toxoplasma gondii. *Parasitology* **97**, 1–10
82. Herm-Gotz, A. (2002) Toxoplasma gondii myosin A and its light chain: a fast, single-headed, plus-end-directed motor. *EMBO J.* **21**, 2149–2158
83. Agrawal, S., van Dooren, G. G., Beatty, W. L., and Striepen, B. (2009) Genetic evidence that an endosymbiont-derived endoplasmic reticulum-associated protein degradation (ERAD) system functions in import of apicoplast proteins. *J. Biol. Chem.* **284**, 33683–33691
84. Anderson-White, B. R., Ivey, F. D., Cheng, K., Szatanek, T., Lorestani, A., Beckers, C. J., *et al.* (2011) A family of intermediate filament-like proteins is sequentially assembled into the cytoskeleton of Toxoplasma gondii. *Cell. Microbiol.* **13**, 18–31
85. Cesbron-Delauw, M. F., Tomavo, S., Beauchamps, P., Fourmaux, M. P., Camus, D., Capron, A., *et al.* (1994) Similarities between the primary structures of two distinct major surface proteins of Toxoplasma gondii. *J. Biol. Chem.* **269**, 16217–16222